

https://dspace.org/

Effect of dispersion of carbon nanotubes on the synthesis of carbon nanotube/ polysulfone composite membranes

Hlanyane, Palesa

2016

http://hdl.handle.net/10539/20059

Downloaded from a DSpace repository. https://dspace.org/



EFFECT OF DISPERSION OF CARBON NANOTUBES ON THE SYNTHESIS OF CARBON NANOTUBE/POLYSULFONE COMPOSITE MEMBRANES

MSc (50/50) RESEARCH REPORT

Palesa Hlanyane

(0412686V)

This is a report submitted to the Faculty of Engineering and the Built Environment, University of the Witwatersrand, Johannesburg, in partial fulfillment of the requirements for the degree of Master of Science in Chemical Engineering (Petroleum Engineering).

07 August 2015

Declaration

I, Palesa Hlanyane, declare that the work in this report is my own unaided effort unless otherwise stated. It has been submitted for the Degree of Master of Science in Chemical Engineering (Petroleum Engineering) at the University of the Witwatersrand, Johannesburg. It has not been submitted for any degree or examination in any other University.

……

Palesa Hlanyane

07 August 2015

Dedication

This work is dedicated to my loving sister, for her continued support and encouragement. I hope that by achieving this milestone, we will grow from strength to strength in the pursuit of happiness, and that we will use our knowledge to change our world for better. This work is also dedicated to my family, friends and mentors for their unfailing love and constant prayers.

"The Lord has never failed and will not start now".

Acknowledgements

I am grateful to my supervisor Dr. Michael Daramola and co-supervisor Professor Sunny Iyuke for dedicating their time in guiding and affording me the opportunity to learn and succeed in my research work. Special thanks to individuals in the supporting facilities and laboratories, internal and external to the University of the Witwatersrand for contributing their knowledge and expertise during characterizing of the membranes, performance evaluation and unpacking my findings. In particular, I would like to thank Oluseyi Abarefa, Jacques Gerber, Prof. Sabelo Mhlanga, Dr Bhekani Mbuli, Lebea Nthinya and Lorenzo LeRay for their time and guidance.

I thank my family, friends and mentors for their support and belief in my ability to succeed in all my endeavors. This research work was made possible by the funding provided by Chemical Industry Education & Training Authority (CHIETA), an organization I would like to acknowledge and express gratitude.

Publications

1. , M.O. Daramola, P. Hlanyane, S. Iyuke, Effect of CNT dispersion methods on the quality and performance of CNT/polysulfone membranes on oil-water mixture separation , Separation Science and Technology (under review).

2. P. Hlanyane, M.O. Daramola, S. Iyuke, Effect of CNT particle size on the performance of CNT/polysulfone membranes on oil-water mixture separation (accepted as a full paper for oral presentation in APCChE2015, 27 September-1 October 2015 Melbourne, Australia)

Abstract

In this study, a Carbon Nanotube (CNT) dispersion method which can be adopted during the synthesis of a CNT/polysulfone Mixed Matrix Membrane (MMM) resulting in optimal performance in the application of oil and water separation is described. Furthermore, the influence of the CNT particle size on MMMs performance is reported. The two aspects of CNT/polysulfone MMMs considered in this study were investigated in two parts. In the first part of this work, CNT/polysulfone MMMs with 5% multi-walled CNT loading and pure polysulfone membranes were synthesized using the phase inversion method, three CNT dispersion methods (Method 1, Method 2 and Method 3 were adopted during synthesis of the MMMs). Characterization of the membranes and CNT was carried out to examine the morphology, the surface chemistry as well as the hydrophilic properties. Scanning Electron Microscopy (SEM) micrographs depicted both porous cross sections and surface morphologies in MMMs and polysulfone membranes. However, the degree of CNTs dispersion within the polysulfone matrix was less pronounced for MMMs prepared using CNT dispersion Method 2. The functional groups observed for the MMMs and CNTs using Fourier Transform Infrared Spectroscopy (FTIR) spectra included carboxylic acid groups (O−H) and carbonyl group (C=O) which are responsible for hydrophilic properties. The contact angles measured for the MMMs using CNT dispersion Method 1, Method 2 and Method 3 were 76.6±5.0°, 77.9±1.3° and 77.3±4.5° respectively, while 88.1±2.1° was measured for the pure polysulfone membranes. The oil rejection obtained for MMMs synthesized by adopting CNT dispersion Method 1, Method 2 and Method 3 were 48.71%, 65.86% and 99.88% respectively. The oil rejection obtained for the pure polysulfone membrane was 84.92%. The pure water and oil water flux increased with an increase in trans-membrane pressure for all the membranes. The oily water permeability of the MMMs

was 26.4 L m^{-2} h^{-1} bar^{-1}, 113 L m^{-2} h^{-1} bar^{-1} and 2.3 L m^{-2} h^{-1} bar^{-1} for MMMs prepared using CNT dispersion Method 1, Method 2 and Method 3 respectively, while the pure polysulfone membrane oily water permeability was 6.9 L m^{-2} h^{-1} bar^{-1} at 6.9 bar.

The competition between water and oil to occupy the porous sites of the membranes was confirmed by the low oil rejection result for M_4, indicating that the surface chemistry of the membranes favours the absorption of oil over water. The low rejection observed for M_1 and M_2 were attributed to poor CNT dispersion and formation of interfacial defects between the CNTs and polymer matrix, resulting in an increase in the free fraction volume that enhanced the permeation flux as well as the permeability. The adoption of CNT dispersion Method 3 has produced MMMs with exceptional oil rejection as well as good permeability.

In the second part of this work, CNT dispersion Method 3 was adopted during the synthesis of MMMs with different CNTs particle size while the CNT loading was kept at 5%. CNT I, OD 6-9 nm **x** L 5 nm, and CNT II, D 110-170 nm **x** L 5-9 μm , were used in the study. Characterisation techniques and performance evaluation methods used in the first part of this work were also employed in part two. FTIR spectra confirmed that the functional groups present in both the CNTs were similar and most importantly included carboxylic acid groups (O−H). The contact angles measured for MMMs from CNT I and CNT II were 77.3 ± 4.5° and 78.8 ± 5.6° respectively. The oil rejection obtained was 99.88% and 99.76% for CNT I MMMs and CNT II MMMs respectively. The oily water permeability was 2.11 L m^{-2} h^{-1} bar^{-1} and 2.20 L m^{-2} h^{-1} bar^{-1} for CNT I and CNT II respectively, at 8.28 bar. Fouling of CNT II MMMs was observed from a

trans-membrane pressure at 9.66 bar which resulted in a decrease in permeability, while the oil permeation flux for CNT I MMMs increased with increasing TMP above 9.66 bar.

This study demonstrates that the CNT dispersion method employed during synthesis influences the performance of MMMs in oil-water mixture separation, as well as the hydrophilic properties, which was indicated by the differences in the MMM contact angles. An interesting observation was that the incorporation of CNT in CNT/polysulfone composites can also be detrimental to the performance of the MMM, which was illustrated by the poor oil rejection obtained for MMMs prepared using CNT dispersion Method 1 compared to the pure polysulfone results. Furthermore, the CNT particle size has been shown to influence the performance of CNT/polysulfone MMMs. Increasing the particle size of the CNTs resulted in improved oil permeation flux as well as permeability at low pressure, however at a TMP above the 8.28 bar, MMMs with bigger CNTs foul more rapidly. The best CNT dispersion can be obtained in CNT/polysulfone MMMs by employing CNT dispersion Method 3 during synthesis and using small CNT diameters.

CONTENTS

Declaration i

Dedication ii

Acknowledgements iii

Publications iv

Abstract v

List of Figures xi

List of Tables xiv

Abbreviations xv

1 Introduction 2

1.1 Motivation and background 2

1.2 Research questions 5

1.3 Aim and objectives 5

1.4 Report layout 6

2 Literature review 8

2.1 Filler dispersion techniques during synthesis of MMMs 8

2.2 The influence of filler particle size on mixed matrix membranes 15

3 Experimental procedure 18

3.1 Method 18

3.2 Membrane synthesis 20

3.2.1 Pure polymer membranes 20

3.2.2 Synthesis of mixed matrix membranes using CNT dispersion Method 1 21

3.2.3 Synthesis of mixed matrix membranes using CNT dispersion method 2 23

3.2.4 Synthesis of mixed matrix membranes using CNT dispersion method 3 24
4 Effect of CNT dispersion on the quality of the synthesized CNT/polysulfone composite membranes 27
4.1 Introduction 27
4.2 Experimental 28
4.2.1 Materials 28
4.2.2 Methods 28
4.3 Results and discussion 33
4.3.1 Physico-chemical characterization of CNT and synthesized membranes 33
4.3.2 Evaluation of membrane performance 53
4.4 Summary 62
5 Effect of particle size of CNTs on the performance of CNT/Polysulfone composite membranes 65
5.1 Introduction 65
5.2 Experimental 65
5.2.1 Materials 65
5.2.2 Methods 66
5.3 Results and Discussion 68
5.3.1 Physico-chemical characterization of CNT and synthesized membranes 68
5.3.2 Evaluation of Membrane Performance 73
5.4 Summary 83
6 Conclusions and recommendations 86
6.1 Conclusions 86

6.2 Recommendations for future studies 87

References 89

Appendices 94

Appendix A Sterlitech membrane test cell system specifications 94

Appendix B SEM micrographs of the membranes 95

Appendix C FTIR spectra of the polysulfone polymer (Sigma Aldrich) 99

List of Figures

Figure 2. 1 Filler dispersion methods which can be adapted during the synthesis of MMMs according to Aroon et al. (2010). (a) filler dispersion Method 1, (b) filler dispersion Method 2 and (c) filler dispersion Method 3 9

Figure 3. 1 Overall MMM synthesis steps, characterisation and performance evaluation procedure. 19

Figure 3. 2 Steps followed during the synthesis of a pure polysulfone membrane. 21

Figure 3. 3 Steps for synthesizing a CNT/polysulfone MMM following CNT dispersion method 1 (Aroon et al., 2010)..... 22

Figure 3. 4 Steps for synthesis of the CNT-polysulfone MMM following CNT dispersion method 2 (Aroon et al., 2010)..... 23

Figure 3. 5 Synthesis of the CNT-polysulfone MMM following CNT dispersion method 3 (Aroon et al., 2010)..... 24

Figure 4. 1 Overall flow diagram of membrane preparation, characterization, and performance evaluation to be employed in evaluating the effect CNT dispersion methods (Aroon et al., 2010). 29

Figure 4. 2 Process flow diagram of the Sterlitech cross flow filtration module. 31

Figure 4. 3 TEM micrographs (a) indicating the morphology of the CNTs at high magnification, (b) indicating structure and ends of the CNTs. 34

Figure 4. 4 (a) TEM micrographs of the CNTs (b) A sample of TEM micrograph indicating lumpy material (Yudianti et al., 2011). 35

Figure 4. 5 (a) SEM micrographs of the cross-sectional view of the polysulfone membrane at high magnification (500 X), showing the thickness of the polysulfone membrane;

(b) SEM micrographs of the polysulfone membrane showing the porous cross-section, (c) indicating the polysulfone membrane surface morphology. 37

Figure 4. 6 SEM micrographs showing the cross-sectional view of the M1 at high magnification (a) (500 X), (b) (10 000X) and (c) (100 000X) showing the surface morphology and the presence of CNTs in the MMM. 40

Figure 4. 7 SEM micrographs of the cross-sectional view of the M2 at high magnification (a) (500 X), (b) (10 000X) and (c) (100 000X), showing the surface morphology and the presence of CNTs in the MMM. 41

Figure 4. 8 SEM micrographs of the cross sectional view of the M3 at high magnification (a) (500X), (b) (10 000X) and (c) (100 000X) showing the surface morphology and the presence of CNTs in the MMM. 42

Figure 4. 9 SEM micrographs indicating the porous cross-section and surfaces of (a) M1, (b) M2, (c) M3 and (d) M4. 44

Figure 4. 10 SEM micrographs showing the cross-sectional area view of the membranes at high magnification for (a) M1, (b) M2, (c) M3 and (d) M4 45

Figure 4. 11 FTIR spectra of (a) CNTs, (b) M1 and (c) polysulfone membrane (M4)..... 47

Figure 4. 12 Structure of the polysulfone polymer (Sigma Aldrich) 49

Figure 4. 13 Pure water flux of M1, M2, M3 and M4 from 1.38 bar to 6.9 bar. 54

Figure 4.14 OWF of the membranes. 57

Figure 4.15 The oil rejection for the membranes. 61

Figure 5. 1 Overall flow diagram for membrane preparation, characterisation, performance evaluation and testing to be employed in evaluating the effect of CNT particle size on MMM performance during oil and water sepration. 67

Figure 5. 2 TEM micrographs of the CNT samples showing (a) CNT I (b) CNT II 68

Figure 5. 3 TEM micrographs of (a) CNT I and (b) CNT II..... 69

Figure 5.4 FTIR spectra analysis of (a) CNT I and (b) CNT II samples. 70

Figure 5. 5 Pure water flux evaluation for M3 and M5. 74

Figure 5. 6 OWF for M3 and M5. 79

Figure 5.7 The average rejection rate for the membranes for the TMP range. 82

List of Tables

Table 4. 1 Average contact angles measured using the sessile drop method. 52

Table 4. 2 The PWP results for M1, M2, M3 and M4 tested using de-ionized water at varying TMP. 55

Table 4. 3 OWP for M1, M2, M3 and M4, M2PR using de-ionized water. 59

Table 5. 1 Measured average contact angles of the membranes..... 72

Table 5. 2 The PWP of M3 and M5 at varying TMP. 75

Table 5. 3 PWF study comparison with previous reports for MMMs prepared by Kim et al. (2013)..... 77

Table 5. 4 The PWP for M3 and M5 tested at varying TMP..... 80

Table 5. 5 The PWP and OWP for M3 and M5 at varying TMP. 81

Abbreviations

C_F	The oil concentration in the feed to the cross flow unit (mg/l) and
C_P	The oil concentration in the permeate (mg/l).
CNT	Carbon Nanotubes
DMF	Dimethylformamide
FTIR	Fourier Transform Infrared Spectroscopy
MF	Micro-Filtration
MMM	Mixed Matrix Membrane
M_1	MMMs prepared using CNT dispersion method 1
M_2	MMMs prepared using CNT dispersion method 2
M_3	MMMs prepared using CNT dispersion method 3 with CNT I
M_4	Pure polysulfone membranes
M_5	MMMs prepared using CNT dispersion method 3 with CNT II
NF	Nano-Filtration
OD	Outer Diameter
OWF	Oily Water Flux
OWP	Oily Water Permeability
PEG	Poly-ethyl glycol
PWF	Pure Water Flux
PWP	Pure Water Permeability
R	Oil rejection
RO	Reverse Osmosis
SEM	Scanning Electron Microscopy

TGA	Thermo-Gravimetric Analyser
TEM	Transmission Electron Microscopy
TMP	Trans-Membrane Pressure
UF	Ultra-Filtration

Chapter One

Introduction

1 Introduction

1.1 Motivation and background

Oil-in-water emulsions are the most serious pollutants in waste water for which current separation technologies are often costly and ineffective (Abadi et al., 2010). Conventional technologies being applied in oil and water separation include emulsion breakers, gravity oil and water separators, American Petroleum Institute (API) separators etc. Using the emulsion breaking technology, oil and water separation is facilitated by the addition of chemicals including sulphuric acid and hydrochloric acid to the emulsified oil and water mixture. However these chemicals are toxic and costly, rendering the technology harmful to the environment and uneconomical due to the additional cost of chemicals required for this technology. Gravity oil and water separation technology is relatively less costly compared to emulsion breaking but it is only effective for bulk removal of free oil and grease and not effective in the removal of emulsified oils in water.

An alternative technology which is gaining interest in the treatment of waste water is membrane technology. The developments in membrane technology have led to scientific breakthroughs in the treatment of wastewater since the discovery of the osmosis phenomenon in natural membranes by Abbe Noilett in 1748 (Kołtuniewicz, 2005). The progress made in membrane technology has led to significant innovation for wastewater treatment, and as a leading process it has influenced the upgrading and expansion of wastewater separation facilities globally. Membrane technology offers unparalleled capability in meeting rigorous effluent and potable water quality requirements, the technology is more economical compared to conventional technologies.

The advantages of membrane technology applications in microfiltration and ultrafiltration include the relatively low energy requirement in operation due to low filtration pressure required and the lack of chemical addition to achieve the required water quality specifications according to Abadi et al. (2010). Membrane filtration is classified into various categories, characterised by separation based on the minimum particle size. Particle size ranging from 0.1–10 μm can be separated using Micro-Filtration (MF), while separation of particles ranging from 0.01–0.10 μm can be achieved with Ultra-Filtration (UF), separation of particles in the order of nanometers can be achieved with Nano-Filtration (NF), and for mono-ionic salts in solution separation can be achieved with Reverse Osmosis (RO) (Maphutha et al., 2013).

Membrane technology can be used as a secondary means of removing dissolved species; organic compounds; phosphorus; nitrogen species; colloidal and suspended solids amongst other pollutants in wastewater. The requirements of a good polymeric membrane include good permeability, selectivity, thermal stability, chemical stability and mechanical strength depending on the application. The various materials used as precursor polymers during synthesis of membranes for filtration applications include polysulfone, poly-ethersulphone, poly-vinidilene fluoride, poly-acrilonitrile, polyamide, aliphatic polyamides, cellulosic and ceramic (Kołtuniewicz, 2005). Pure polymer membranes are somewhat deficient in meeting the requirements of a good membrane technology mainly due to poor mechanical strength as well as poor thermal stability (Aroon et al., 2010). The problems associated with membranes technology include concentration polarization and fouling. Concentration polarization is caused by the formation of a layer on the membrane resulting from accumulation of impermeable or slow permeating particles while fouling is caused by the deposition of organic substances, colloids, biological growth and scaling on the membrane (Maphutha et al., 2013). During membrane

synthesis, the adverse impact of fouling and concentration polarization on the performance of the membrane should be considered and the best method adopted to decrease fouling of the membrane while maintaining the highest performance.

In order to overcome some of the limitations posed by pure polymeric membranes, research has been focused on Mixed Matrix Membranes (MMMs). MMMs are prepared by dispersing porous particles, such as Zeolites, Carbon Molecular Sieves (CMS), Silica and Carbon Nanotubes (CNTs) within the polymer matrix, these porous particles are also referred to as fillers (Aroon et al., 2010). The presence of the porous nano particles in the polymer matrix have been reported to enhance the thermal stability (Aroon et al., 2010) and mechanical strength of MMMs when compared to pure polymeric membranes by Maphutha et al.(2013). Maphutha et al (2013) has further reported that MMMs with CNTs as fillers, when used in the application of oil and water separation surpass the performance of pure polymeric membranes. In previous studies conducted by Abadi et al. (2010), Chakrabarty et al. (2008), Ebrahimi et al. (2009), Mondal and Wickramasinghe (2008) and Yi et al. (2011), encouraging results were obtained using MMMs in the application of oil and water separation. However, one of the main problems associated with MMMs is the poor adhesion and dispersion of the filler in the polymer matrix (Aroon et al., 2010).

The aim of this study was to add to the advancement of knowledge of MMMs, in particular polysulfone/CNT MMMs, in the application of oil and water separation.

1.2 Research questions

The study seeks to understand and add to the knowledge of the application of CNT/polysulfone MMMs in oil and water separation by addressing the following questions.

i. Which CNT dispersion method will lead to an improved CNT dispersion in the polysulfone matrix that will result in a high performing CNT/polysulfone MMMs during oil-water mixture separation?
ii. What is the impact of CNTs particle size on the performance of CNT/polysulfone MMMs during oil-water mixture separation?

1.3 Aim and objectives

The aim of this study is to determine the best CNT dispersion method to be adopted during the synthesis of CNT/polysulfone MMMs and also examine the effect of CNT particle size on the performance of the MMMs in the separation of oil and water mixtures. In order to address the research questions posed in section (1.2), the following objectives were defined:

i. Synthesis of CNT/polysulfone MMMs by using three (3) CNT dispersion methods,
ii. Characterisation and evaluation of the membrane performance during oil-water mixture separation.
iii. Study the effect of particle size of CNTs on the synthesis of CNT/polysulfone ,
iv. Investigate the performance of the synthesized MMMs using oil-water mixture separations.

1.4 Report layout

The research layout of this report is outlined below:

Chapter 1 is the introductory section of this study and provides the background to MMMs in the application of oil-water mixture separation. In addition, it reports the aim and objectives of this study.

Chapter 2 provides the literature review of previous studies on CNT dispersion methods employed during membrane synthesis as well as previous studies on the effect of filler size on polymeric MMMs.

Chapter 3 describes the experimental procedure adopted in this study. The details of the methods used to prepare the membranes were provided in this chapter.

Chapter 4 discusses the effect of CNT dispersion on the quality and performance evaluation of the synthesized CNT/polysulfone composite membranes during oil-water mixture separation. The results of characterization of the membranes are also provided and discussed.

Chapter 5 discusses the effect of particle size of CNTs on the quality and performance of CNT/polysulfone composite membranes. The results of characterization of the membranes are also provided and discussed.

Chapter 6 summarises the conclusions which have emanated from the analyses of the results obtained and recommendations for future studies.

Chapter Two

Literature review

2 Literature review

2.1 Filler dispersion techniques during synthesis of MMMs

MMMs comprising of rigid porous nanoparticles such as zeolites, carbon molecular sieves, silica and carbon nanotubes, dispersed in a continuous polymeric matrix present an interesting approach for improving the separation properties of polymeric membranes (Aroon et al., 2010). Aroon et al. (2010) studied the performance of MMMs in gas separation applications as well as various CNT dispersion methods which can be adopted during the synthesis of MMMs. Their review provided an overview of the effect of the dispersed phase on membrane performance, the effect of filler and polymer interfacial defects on membrane properties, MMM synthesis methods to be aid in avoiding interfacial defects and the effect of particle size on MMMs performance. The subjects of interest in this study are the filler dispersion methods adopted during MMM synthesis and the effect of filler particle size on the performance of the MMM. The various filler dispersion methods which can be adopted during MMM synthesis according to Aroon et al. (2013) are the following:

i. Dispersion of filler particles in a solvent, followed by stirring and addition of the polymer into the homogenous suspension.
ii. Dissolving the polymer in the solvent by stirring for a predetermined duration, followed by the addition of filler particles in the polymer solution.
iii. Dispersion of filler particles in a solvent followed by stirring for a predetermined duration and preparation of polymer solution separately by dissolving the polymer into the solvent and stirring for a predetermined time. Addition of the filler particle suspension and polymeric solution.

The suggested filler dispersion methods to be adopted during the synthesis of the MMMs are schematically depicted in Figure 2.1.

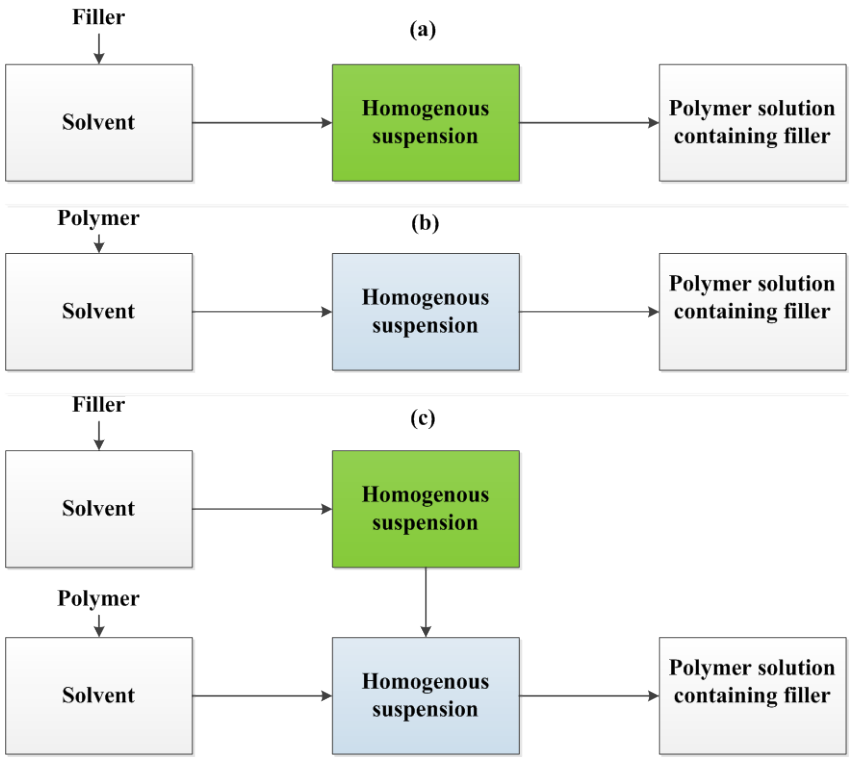

Figure 2. 1 Filler dispersion methods which can be adapted during the synthesis of MMMs according to Aroon et al. (2010). (a) filler dispersion Method 1, (b) filler dispersion Method 2 and (c) filler dispersion Method 3

CNT dispersion Method 2 was adopted by Maphutha et al. (2013) during the synthesis of a CNT infused polysulfone MMM with a Poly-Vinyl Alcohol (PVA) layer which was later used for the separation of oil and water. The incorporation of pristine CNT as a filler in the polysulfone matrix resulted in an increase in the mechanical strength of the MMM when compared to the pure polysulfone membrane as reported by Maphutha et al. (2013). However, a decline in mechanical strength of the CNT/polysulfone MMM was observed at CNT concentration above 7.5%. This decline was attributed to the re-agglomeration of CNTs in the polymer matrix

(Maphutha et al., 2013) resulting from poor adhesion and interfacing of the CNT and polysulfone. To prevent interfacial defects between the filler and polymer during MMM synthesis, particularly for MMMs with CNT used as filler, CNT priming has been proposed by Aroon et al. (2010). Priming is a method that involves coating the surface of the filler with a diluted polymer dope prior to dispersion in the bulk polymer, thereby reducing the stress at the polymer and filler interface as particles are mixed in a suitable solvent and small amount of polymer, with a polymer layer formed around the filler (Aroon et al., 2010). In addition, the priming technique was reported to enhance the interaction between the bulk polymer and polymer primed particles, thereby minimizing defective particle-polymer interfaces according to Aroon et al. (2010). However, priming requires that the filler material be evenly dispersed in the solvent prior to addition of the polymer to prevent priming of filler agglomerates.

Zhao et al. (2014a) showed that the incorporation of functionalised Multi Walled Carbon Nanotubes (MWCNT) in a polyamide layer by interfacial polymerization resulted in improved antifouling properties of their membranes when compared to pure polyamide membranes. Zhao et al. (2014a) synthesized MMMs by adopting CNT dispersion Method 1 and varied the MWCNT loading in the polyamide matrix. Salt rejection in excess of 90% was reported in the study for the MMMs.

In the study conducted by Ma et al. (2010), the interaction between carbon nanotubes and polymers was critically reviewed. The principles and techniques for CNT particle dispersion, CNT functionalization and the effects of CNT dispersion on the properties of CNT/polymer nano-composite were reviewed. The CNT dispersion methods which were reviewed include

ultrasonication, shear mixing, cal-endaring, ball milling, and stirring. Ultrasonication is the most commonly used method for the dispersion of nanoparticles in a polymer matrix, and was used for dispersing CNTs in the preparation of the CNT-polysulfone MMM with a PVA layer by Maphutha et al. (2010). Ultrasonication generates waves which serve as a means of separating the nanoparticles at the surface, leading to separation of individualized nanoparticles from the bundles. According to Ma et al. (2010), ultrasonication is an effective method for dispersing nanoparticles in liquids with relatively low viscosity such as water. However the method is not effective in liquids with a high viscosity such as polymers which suggests that CNT dispersion Method 2 is preferable over Method 1. To increase the effectiveness of nanoparticle dispersion, dilution of the polymer with a solvent is recommended when using ultrasonication. Ma at el. (2010) further recommended the use of solvents to be considered in a cold ultrasonication bath due to the operating principle of ultrasonication, which often results in elevated temperatures of the solution which can lead to re-agglomeration of the CNTs. The noted disadvantage with ultrasonication was that it can lead to damage of the nanoparticles and in order to minimize the defect of the nanoparticles, the exposure time should be limited. The calender, or commonly known as three roll mills, is a machine tool that employs shear force created by rollers to mix, disperse or homogenize viscous materials and was used previously by Ma et al. (2010) as a CNT dispersion method. The calender method was reported not to be effective in the dispersion on the CNT in the polymer matrix due to disparities in the gap size between the rollers and the diameter of the CNTs. It was reported that dispersed CNTs and the agglomerates co-existed in the nanocomposites after calendaring. Ma et al. (2010) described stirring as a technique which can be adopted for dispersing CNTs in a polymer but in order to prevent re-agglomeration of the CNTs in the polymer matrix, high shear forces were recommended, which can be achieved by

employing high mixing speeds. Comparing the various CNT dispersion methods which were reviewed by Ma et al. (2010), ultrasonication has the disadvantage of potentially damaging the CNT structure if exposure is prolonged, whereas calendaring and stirring will not damage the CNT during the MMM preparation stage.

In a study conducted by Cooper et al. (2002), polymer nanocomposites consisting of various CNT and nanofibrils loading in a Poly-Methyl Methacrylate (PMMA) matrix were prepared using a polymer extrusion technique. Cooper et al. (2002) reported that ultrasonication is not sufficient if used solely for the dispersion of CNT in a polymer nanocomposite. Additional preparation of the CNT and polymer is required in order to obtain even distribution of CNTs in the polymer matrix. In this case, mixing the polymer and CNT particles by grinding powder prior to preparing the membrane was reported to be effective in dispersing the CNT particles in the MMM.

In a study done by Yang and Xie (2011), the effect of functionalisation of CNTs on the dispersion and adhesion on the polymer matrix was conducted. According to Yang and Xie (2011), in order to optimise the mechanical strength of the polymer nanocomposite, the interfacial bonding of the CNTs on the polymer surface is important which was also suggested by Aroon et al. (2010). The study mainly focused on the effect of functionalisation of CNTs prior to incorporation in the polymer matrix by both the non-covalent wrapping method and chemical bonding between functional molecules and CNTs. Yang and Xie (2011) reported that CNTs are excellent candidates for substituting or complementing conventional nanofillers in the synthesis of multifunctional polymer nanocomposites owing to their unique electronic, thermal and

mechanical properties. Similar to most studies done for CNT/polymer composites, the main challenge was found to be CNTs dispersion in polymers matrices to achieve good matrix/nanotube adhesion that maximizes the transfer of the nanotube properties to the polymer matrix.

The dispersion methods and the alignment of CNTs in a polymer nanocomposites using various techniques was studied by Xie et al. (2005). The methods they studied for the dispersion of CNTs include blending, in situ polymerization and chemical functionalization, ex situ techniques, force and magnetic fields, electro spinning and liquid crystalline phase-induced methods. They also reviewed CNTs blending by high energy sonication, high speed stirring, and also the addition of a compatibiliser to the CNT polymer mixture to ensure proper dispersion of the CNT in the polymer matrix. Xie et al. (2005) reported that the addition of compatibilisers and surfactants, in conjunction with melt blending is effective and can be widely used to enhance the dispersion and interfacial bonding of CNTs in CNT/polymer composites. They recommended CNT chemical functionalisation as an adequate technique to promote good dispersion in the CNT/polymer composites and reported that it could have a dominant role in future development and applications of these nanocomposites.

In the study carried out by Alzahrani et al. (2013), the potential tertiary treatment of produced water using highly hydrophilic Nanofiltration (NF) and Reverse Osmosis (RO) membranes was studied. Alzahrani et al. (2013) reported that RO membranes have greater potential in the treatment of waste water for use as potable water, and NF membranes have the potential to be used in waste water treatment for the reduction of water turbidity, TDS, TSS, Oil and grease,

TOC, conductivity and COD in waste water. The hydrophilic property of the membranes without incorporation of CNT appears to play a major role in the separation properties of the membranes as demonstrated by the good separation efficiency for TDS, TSS, Oil and grease, TOC, conductivity and COD.

In a study reported by Abadi et al. (2010), α-Al_2O_3 Macro Filtration (MF) membrane performance was evaluated using a cross flow filtration for the separation of oil and water using a sample taken downstream of an API separator. A conventional biological treatment method was used in the plant for the removal of TSS, oil and grease, TOC's and also turbidity of the water downstream of the API separator in order to meet the national effluent water standards. The study was done in order to compare the performance of the conventional biological treatment method used for the removal of TSS, oil and grease, TOC's and also turbidity to that of the α-Al_2O_3 MF. The α-Al_2O_3 MF membrane exhibited improved mechanical strength, thermal resistance, chemical resistance and it could be operated in a wide pH range when compared to pure organic membranes used in similar applications (Abadi et al., 2010). Similar to arguments by Alzahrani et al. (2013), α-Al_2O_3 MF membranes were viewed to be suitable for oily waste water treatment due to their hydrophilic surfaces which were reported to contribute to anti-fouling properties of membranes, a major contributor to the effectiveness of membranes in waste water treatment applications. Analysis of waste water for TSS, oil and grease, TOC's and turbidity done before and after treatment showed that the α-Al_2O_3 MF membrane was more effective in treatment compared to the conventional biological treatment method (Abadi et al., 2010).

In the study by Ebrahimi et al. (2009), the characterisation and application of different ceramic membranes for oil-field produced water treatment was studied using varying Al_2O_3 pore size and TiO_2 membranes. They reported oil rejection of 99.5% when using a combination of UF and NF membranes. In a study reported by Chakrabarty et al. (2010), the performance of polysulfone membranes coated with Poly-vinylpyrrolidone (PVP) and Polyethylene Glycol (PEG) in the separation of oil and water were evaluated. The coating of the polysulfone with PEG, which was reported to enhance the hydrophilic property of the membranes, resulted in oil rejection higher than 90% for synthetic oil and water emulsions. The prevailing learning from literature is that the hydrophilic property of the membrane plays a significant role in determining the membrane selectivity and rejection in the application of waste water treatment.

The subject of interest which forms part of this study was to determine the optimum CNT dispersion method, CNT dispersion methods described by Aroon et al. (2010) were adapted as part of this study, to determine the optimum CNT dispersion method. The prepared MMMs were evaluated in the application of oil and water separation similar to previous studies by Ebrahimi et al. (2009), Chakrabarty et al. (2010) as well as Maphutha et al., (2013).

2.2 The influence of filler particle size on mixed matrix membranes

As part of this study, the effect of CNT particle size on the performance of CNT/polysulfone MMM was evaluated. Previous work that reported on the effect of fillers in polymeric membranes is briefly reviewed. Yang and Xie (2011) reported that one of the factors which have an effect on the improvement of MMMs from a structural perspective is smaller CNT diameters. Yang and Xie (2011) identified smaller diameters of CNTs are required to produce a higher packing density but the size range was not specified.

In a review by Aroon et al. (2010), CNT particles size was reported to influence the polymer-nanoparticle interfacial bond. According to Aroon et al. (2010), the polymer-nanotube interfacial contact is influenced by the particle size of the filler used during preparing of the polymeric matrix. The use of nanoparticles less than 20 nm in size was recommended as a reasonable particle size which can enhance the filler/polymer interface. Aroon et al. (2010) recommendation with regard to filler particle size is in agreement with Yang and Xie (2011).

In a study conducted by Tantekin-Ersolmaz et al. (2000) the effect of zeolite particle size on the performance of zeolite/polydimethylsiloxane mixed matrix membranes was investigated. Tantekin-Ersolmaz et al. (2000) reported that as the particle size increases, the permeability of the MMMs increased as well. However, permeability values corresponding to high zeolite loading were similar to those reported for the lower zeolite loading for bigger particle sizes. Tantekin-Ersolmaz et al. (2000) further reported that the particle size does not significantly influence the gas selectivity of the MMMs prepared in their study.

In the study conducted by Ebrahimi et al. (2009), it was reported that an oil rejection of 93% using ceramic membranes, alumina particle size of 0.1 μm and 98% was obtained using alumina with a particle size of 0.05 μm. Ebrahimi et al. (2009) indicated that an increase in filler particle size can result in a decline in oil rejection.

Chapter Three

Experimental Procedure

3 Experimental procedure

3.1 Method

The aim of the study was to investigate the effect of three dispersion methods on the quality of CNT/polysulfone MMMs and the effect of CNT particle size on the quality of the MMMs and their performance in separating emulsified oil and water. In order to achieve these objectives, samples of pure polymer membranes and CNT/polysulfone MMMs were prepared by the phase inversion method, and the MMMs were fabricated according to three CNT dispersion methods adapted from study by Aroon et al. (2010).

The first part of this study focused on determining the best CNT dispersion method out of three during the synthesis of MMMs. The criterion for selecting the best CNT dispersion method was based on the performance of the synthesized CNT/polysulfone MMMs during the separation of oil and water. The second part of this study focused on evaluating the effect of the CNT particle size on the performance of the MMM prepared using the CNT dispersion method established in part one of this study.

The overall experimental steps including MMM fabrication, characterization and performance evaluation are depicted in Figure 3.1.

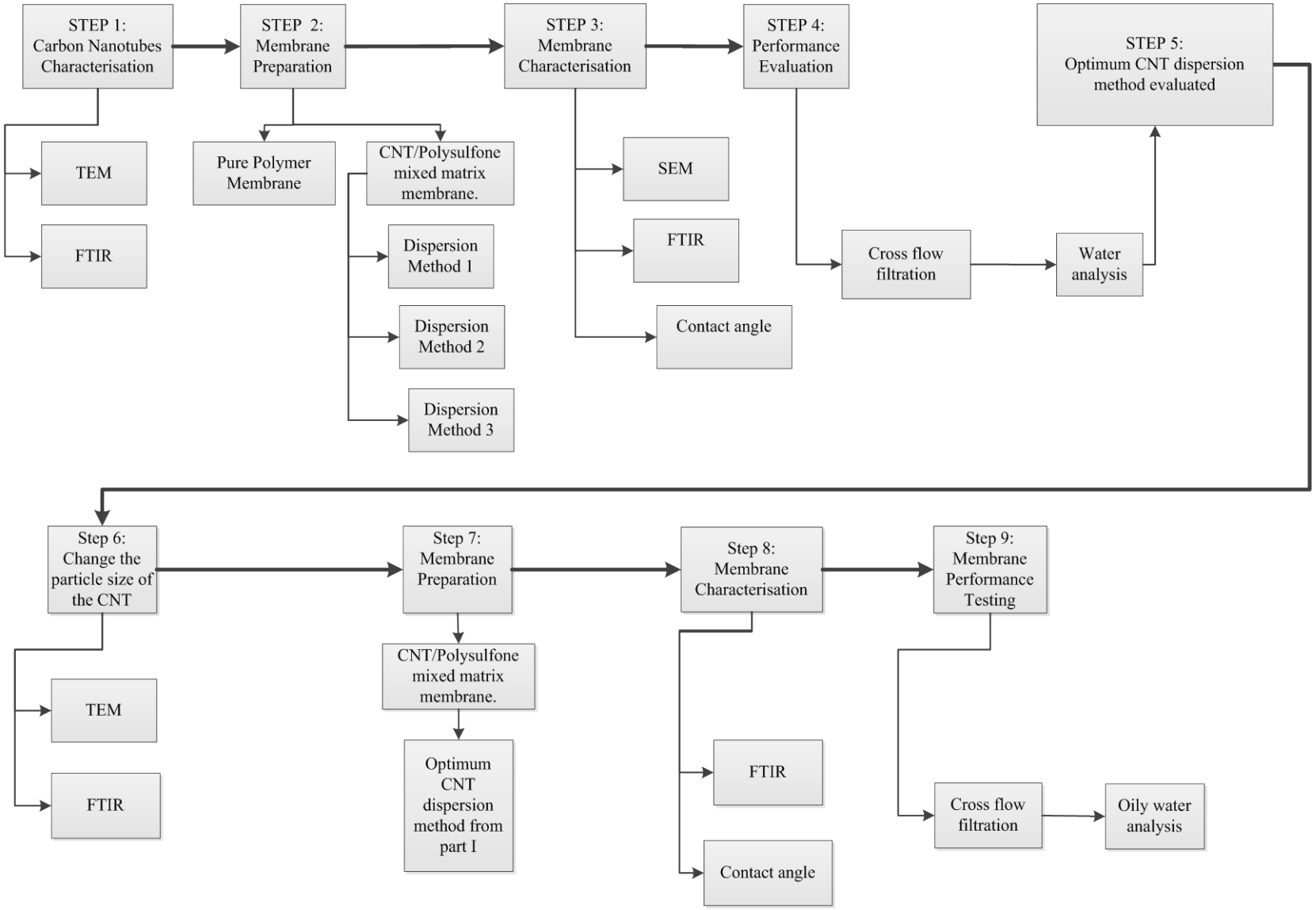

Figure 3. 1 Overall MMM synthesis steps, characterisation and performance evaluation procedure.

In step 1, the CNTs samples were characterized using Transmission Electron Microscopy (TEM) and Fourier Transform Infrared Spectroscopy (FTIR). The second step, Step 2, entailed the synthesis of pure polymer membranes and the MMMs using the three CNT dispersion methods. The morphology of the membranes was determined using SEM and the surface chemistry examined using FTIR. Step 4, which is membrane performance evaluation, entailed testing membranes using a cross flow filtration unit. Based on the results obtained from Step 4, the best CNT dispersion method was adapted to reproduce MMMs using a different particle size CNT in Step 7.

3.2 Membrane synthesis

3.2.1 Pure polymer membranes

A pure polysulfone membrane was prepared as a reference for comparing the MMMs and to investigate the effect of the CNT addition in the polymer matrix. The steps involved in the synthesis of the polysulfone membrane are schematically depicted in Figure 3.2.

A polymer and solvent solution were prepared by mixing 10 g of polysulfone in 50 ml of Dimethylformamide (DMF) and the solution was mixed with a magnetic stirrer for 24 hours. The mixture was then cast on a glass plate and immersed in a distilled water bath for 24 hours to allow for the desorption of the solvent from the membrane, a phenomena known as phase inversion (Maphutha et al., 2013).

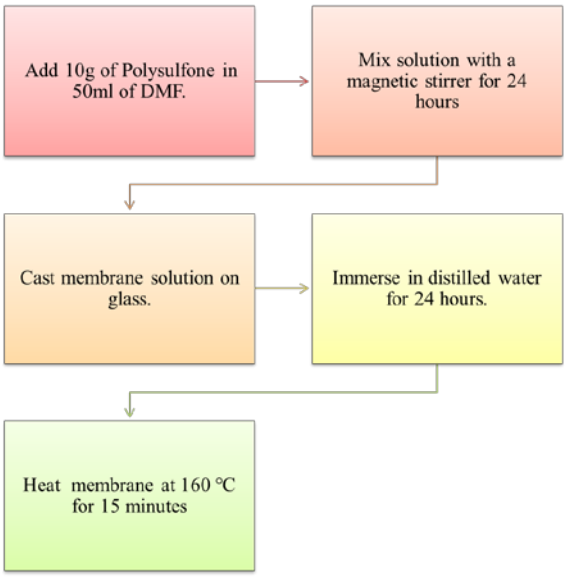

Figure 3. 2 Steps followed during the synthesis of a pure polysulfone membrane.

The membrane was heated in an oven at 160 °C for 15 minutes (see Figure 3.2). The heating of the membrane was done to evaporate the water and the solvent from the membrane as the boiling point of solvent is 153°C.

3.2.2 Synthesis of mixed matrix membranes using CNT dispersion Method 1

The steps for the MMM preparation using CNT dispersion Method 1 is schematically depicted in Figure 3.3. MMM synthesis adapting CNT dispersion Method 1 involved the dispersion of CNTs in DMF and stirring for a predetermined period of time prior to adding the polymer into the suspension.

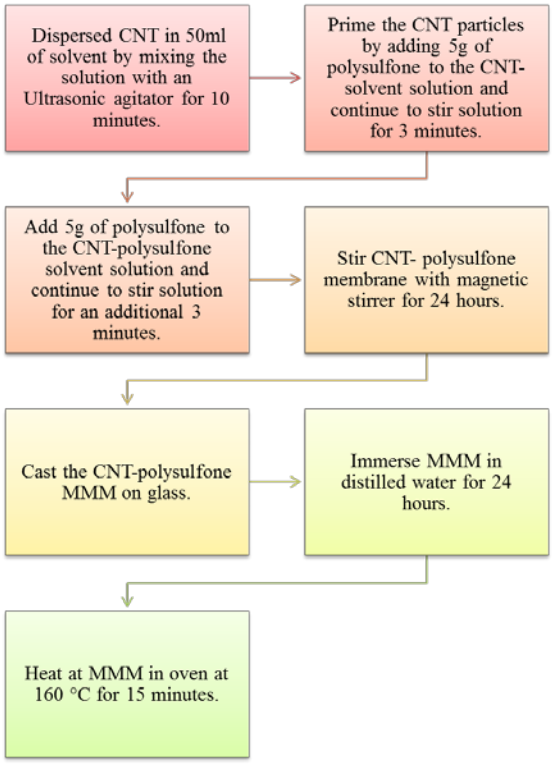

Figure 3. 3 Steps for synthesizing a CNT/polysulfone MMM following CNT dispersion method 1 (Aroon et al., 2010).

CNTs were dispersed in the solvent by mixing the solution using a ultrasonic agitator. After 10 minutes of mixing, 5 g of polysulfone was added to the CNT-solvent solution to prime the particles, and the mixing was continued for a further 3 minutes. After 3 minutes, 5 g of polymer was added to the mixture and the solution was mixed for an additional 3 minutes using the ultrasonic agitator. The CNT/polysulfone mixture was further mixed with a magnetic stirrer for 24 hours (see Figure 3.3). The mixture was cast on a glass plate then immersed in a distilled water bath for 24 hours to allow for the desorption solvent from the MMM, which is known as phase inversion. The membrane was heated in an oven at 160 °C for 15 minutes.

3.2.3 Synthesis of mixed matrix membranes using CNT dispersion method 2

In this method, the polymer was dissolved in the solvent and mixed and then the CNTs were added to the polymer-solvent mixture. The steps for the MMM preparation using CNT dispersion Method 2 is schematically depicted in Figure 3.4.

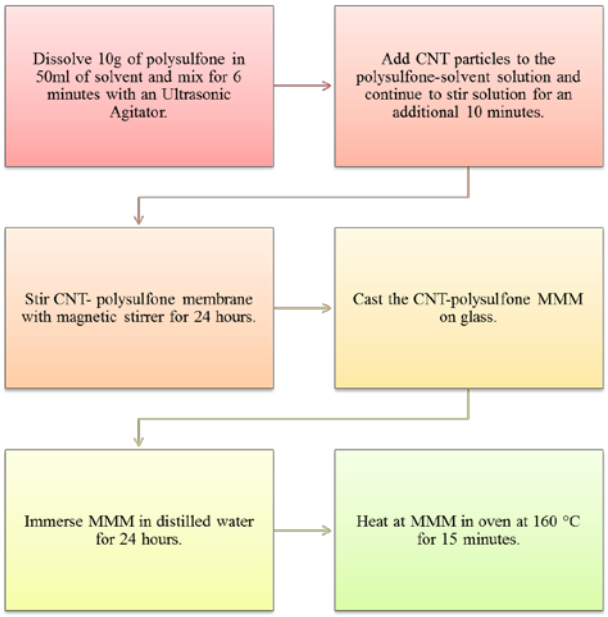

Figure 3. 4 Steps for synthesis of the CNT-polysulfone MMM following CNT dispersion method 2 (Aroon et al., 2010).

About 10 g of polysulfone was dissolved in 50 ml of solvent by mixing with using the ultrasonic agitator for 6 minutes. CNTs were dispersed in the polysulfone-solvent mixture by mixing the solution with the ultrasonic agitator for a further 10 minutes, see Figure 3.4. The CNT-polysulfone mixture was further mixed with a magnetic stirrer for 24 hours. The mixture was

cast on a glass plate then immersed in distilled water for 24 hours to allow for the desorption solvent from the MMM. The membrane was heated in an oven at 160°C for 15 minutes.

3.2.4 Synthesis of mixed matrix membranes using CNT dispersion method 3

In this method, polymer was dissolved in the solvent and stirred for a predetermined time, and then the CNTs were dispersed in the solvent and mixed for a specified time. The two solutions were mixed for a predetermined period. The steps for the MMM preparation using synthesis Steps 3 is schematically depicted in Figure 3.5.

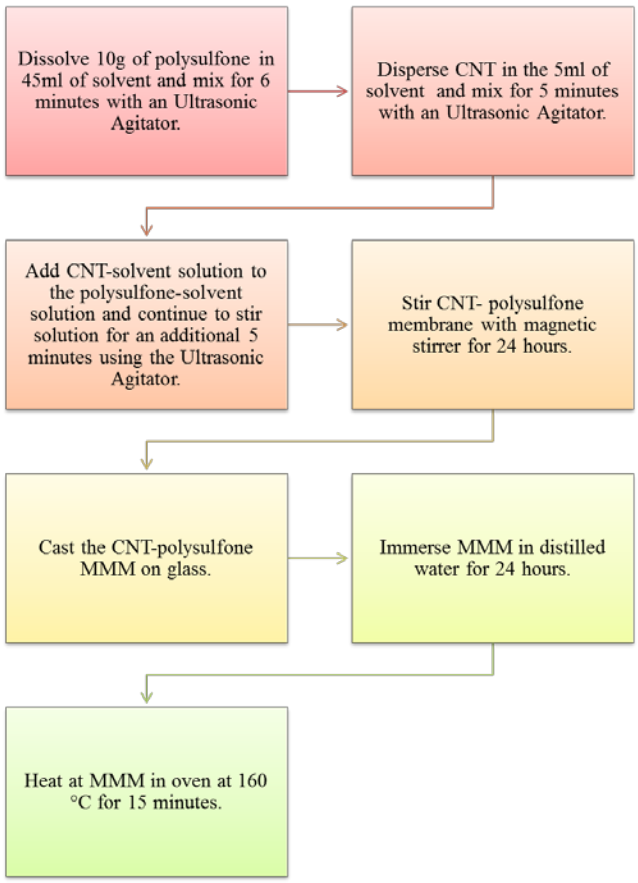

Figure 3. 5 **S**ynthesis of the CNT-polysulfone MMM following CNT dispersion method 3 (Aroon et al., 2010).

About 10 g of polysulfone was dissolved in 45 ml of solvent and mixed with an ultrasonic agitator for 6 minutes. CNTs were dispersed in the solvent by mixing with an ultrasonic agitator for 5 minutes. The two solutions were mixed together in one glass beaker and further mixed with the ultrasonic agitator for 5 minutes then with magnetic stirrer for 24 hours, see Figure 3.5. The mixture was cast on a glass plate and then immersed in a distilled water bath for 24 hours to allow for desorption of the solvent from the MMM. The membranes were heated in an oven at 160°C for 15 minutes.

Chapter Four

Effect of CNT dispersion on the quality and performance of the synthesised CNT/polysulfone composite membranes

4 Effect of CNT dispersion on the quality of the synthesized CNT/polysulfone composite membranes

4.1 Introduction

MMMs are gaining interest in the application of wastewater treatment due to the enhanced membrane properties including mechanical strength, permeability, and selectivity when compared to pure polymeric membranes. MMMs have been prepared previously by dispersing porous particles, such as zeolites, carbon molecular sieves (CMS), silica and carbon nanotubes (CNTs) within the membrane polymer matrix.

MMMs infused with CNTs have been reported to be highly effective when used in the application of oil and water separation. However due to the challenges encountered during MMM preparation, mainly poor dispersion of the CNTs in the polymer matrix, the commercial application of MMMs is limited.

This chapter focuses in the determination of an optimum CNT dispersion method out of the three methods. This was achieved by synthesizing MMMs samples, characterising and evaluating their performance in oily water separation. In this chapter, the materials used, the methods adopted in preparing the membranes, the results and discussion as well as the summary of the findings are described.

4.2 Experimental

4.2.1 Materials

The materials used to prepare the membranes were polysuflone, DMF and CNTs purchased from Sigma Aldrich. The polysulfone polymer supplied was in beaded form with molecular weight specified to be 22 000 g/mol and DMF with molecular weight specified as 73.09 g/mol. According to the supplier, the CNTs used in this work were specified as having an Outer Diameter (OD) 6-9 nm, length of 5 μm and a carbon basis greater than 90%. The CNTs used in this chapter were referred to as CNT I throughout the study.

4.2.2 Methods

MMMs were prepared using CNT dispersion method 1, method 2 and method 3 adopted by Aroon et al. (2010), with a CNT loading of 5% standard for all prepared MMMs. Details of the CNT dispersion methods are reported in Chapter 3. A pure polysulfone membrane was also prepared as a basis for comparison with the MMMs.

The process steps followed for preparing the membranes is depicted in Figure 4.1. The first step entailed the characterisation of the CNT particles using TEM and FTIR, followed by step 2 which entailed the preparation of the polysulfone membrane and the MMMs using the three CNT dispersion methods. Following membrane preparation, membrane characterisation was achieved by SEM, FTIR and also the evaluation of the contact angle (see Figure 4.1). Step 4 entailed membrane evaluation tests as well as the water analysis which was used to determine the optimum CNT dispersion method in step 6, the last step in this chapter.

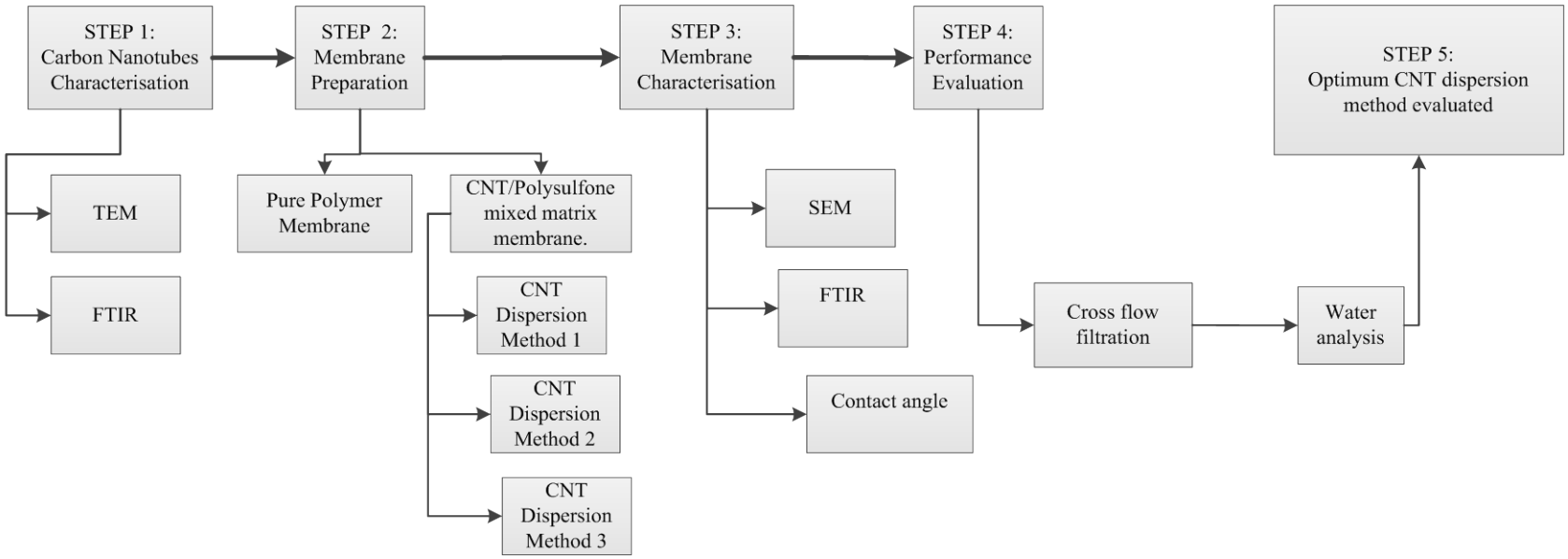

Figure 4. 1 Overall flow diagram of membrane preparation, characterization, and performance evaluation to be employed in evaluating the effect CNT dispersion methods (Aroon et al., 2010).

CNTs were characterised using TEM to evaluate the size and morphology. FTIR was used to examine the functional groups present on the CNTs. The MMM samples were characterised using FTIR to examine for the presence of the CNTs in MMMs. Additionally, the contact angle of the MMMs was evaluated using the Sessile drop method with deionized water to quantify the hydrophilicity of the membranes. The performance of the MMMs in oily water separation was evaluated using the Sterlitech cross flow filtration module (see Figure 4.2).

The Sterlitech cross flow filtration module process equipment included the feed tank, pump, filtration cells, chiller unit, and flow and pressure instruments. A high speed stirrer was used in the feed tank to maintain a homogenous emulsion of oil and water during testing of the oily water. The pump was used to transfer water from the feed tank to the filtration cells where the membranes were fitted during operation. The module has 4 filtration cells which can be used during operation. Permeate from the cell can be circulated back to the tank via flexible hoses or can be routed to measuring beakers for readings during operation. For overpressure protection, a pressure regulating valve set at a 1000 psi is fitted downstream of the pump. Pressure sensors are fitted upstream and downstream of the filtration cells to determine the TMP during operation. The chiller unit was used to control the pump temperature and the drain valve used to discharge the feed tank to a bucket. The control valves were used to set the desired pressure by throttling the pump discharge. The manufacturer's details of the cross flow filtration module are provided in Appendix A. The Pure Water flux (PWF), Pure Water Permeability (PWP), Oily Water Flux (OWF), Oily Water Permeability (OWP) and Oil Rejection (R) were evaluated as reported elsewhere (Masuelli, 2003; Sadeghi, 2013; Yu et al. , 2013; Maphutha et al., 2013; Amini et al., 2013, Yin et al., 2013).

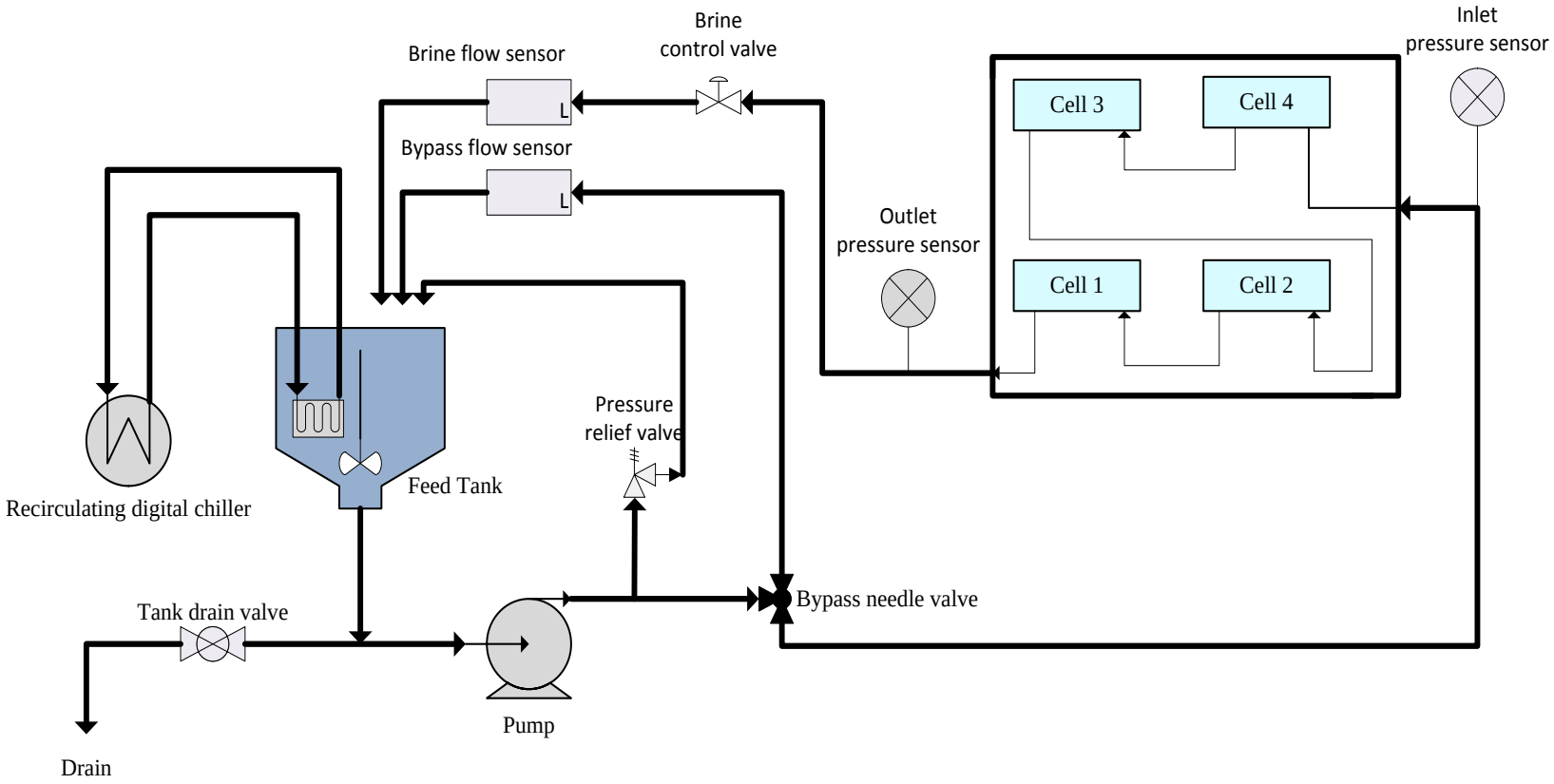

Figure 4. 2 Process flow diagram of the Sterlitech cross flow filtration module.

The PWF and OWF, PWP and OWP as well as the Rejection (R) were determined using Equations (4.1), (4.2), and (4.4) respectively, at various Transmembrane Pressure (TMP) calculated using Equation (4.3):

$$F = \frac{V}{A} \tag{4.1}$$

F is the permeate flux (L m^{-2} h^{-1}), V is the volumetric flow (L.h^{-1}) and A the effective membrane area (m^2).

$$P = \frac{F}{TMP} \tag{4.2}$$

P is the permeability (L m^{-2} h^{-1} bar^{-1}) and TMP is the transmembrane pressure (bar) which is expressed in Equation (4.3).

$$TMP = \frac{P_1 + P_2}{2} \tag{4.3}$$

P_1 (bar) and P_2 (bar) is the measured upstream and downstream pressure of the membranes during operation.

$$R = \frac{(C_F - C_P)}{C_F} \tag{4.4}$$

R is the membrane oil rejection, C_F is the oil concentration in the feed to the cross flow unit (mg/l) and C_P is the oil concentration in the permeate (mg/l).In order to distinguish the

membranes used in the study, the following notations were used to identify the MMM samples as well as the polysulfone membrane as follows:

M_1 Refers to membranes which were prepared using CNT dispersion Method 1.

M_2 Refers to membranes which were prepared using CNT dispersion Method 2.

M_3 Refers to membranes which were prepared using CNT dispersion Method 3.

M_4 Refers to pure polysulfone membranes.

4.3 Results and discussion

4.3.1 Physico-chemical characterization of CNT and synthesized membranes

The physico-chemical characterization of the CNTs using TEM micrographs has been used previously by Slobodian et al. (2012) to determine the morphology of CNTs. They showed that TEM micrographs are suitable in evaluating the structure and physical properties of CNTs. In previous studies by Misra et al. (2007) and Ahmad et al. (2014), TEM was used to characterise multi-walled CNTs. Hence a similar approach was adopted in this study to examine the morphology of the CNTs using TEM micrographs. CNT samples were examined using the FEI Technai TEM operated at a voltage of 120 kV. The TEM micrographs for CNT I samples are depicted in Figure 4.3.

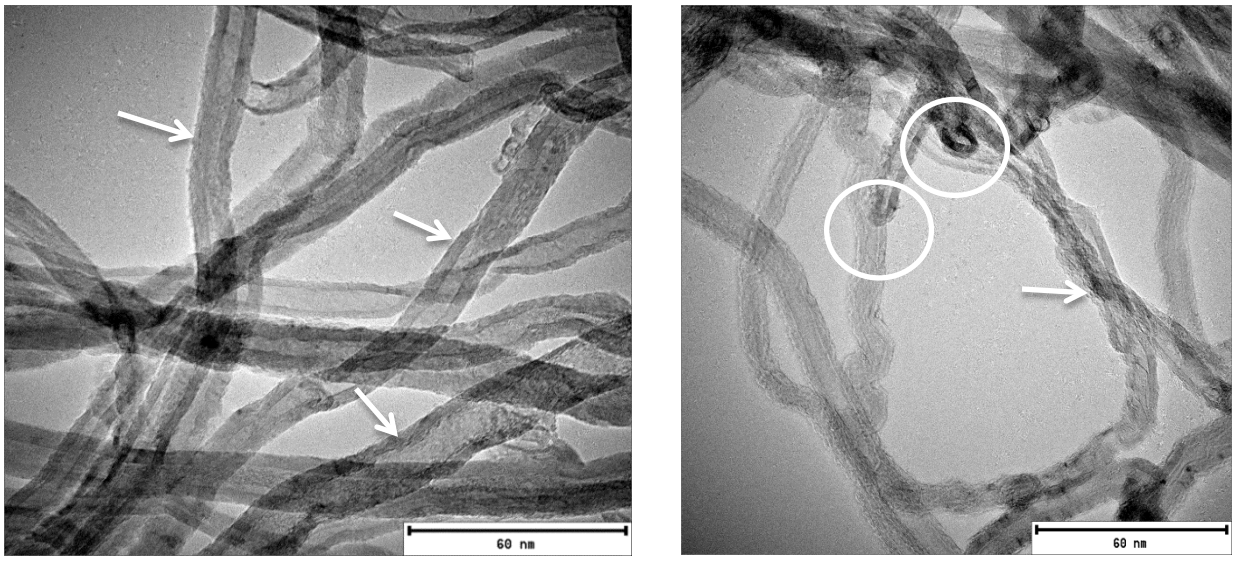

(a) (b)

Figure 4. 3 TEM micrographs (a) indicating the morphology of the CNTs at high magnification, (b) indicating structure and ends of the CNTs

The TEM micrographs indicate the entanglement of the membranes as depicted in Figure 4.2 (a) which is similar to the findings of Ahmad et al. (2014) in the morphology of their of multi-walled CNTs samples. CNT defects are shown on the internal and external surface of the CNTs (see Figure 4.3 (b)). Furthermore, close-ended structures of the CNTs were observed, close ended structures were previously reported by Ahmad et al. (2014) for untreated MWCNTs. In the investigation carried out by Prolongo et al. (2012), the TEM micrographs of pristine MWCNTs showed that untreated CNTs had closed ended structures when compared to amino functionalised CNTs. Surface defects were observed in this study for the CNTs samples as depicted in Figure 4.3 (b).

Further analysis of the CNTs TEM micrographs indicates lumpy material adhering to the CNTs surface as revealed in Figure 4.4 (a), encircled on the image.

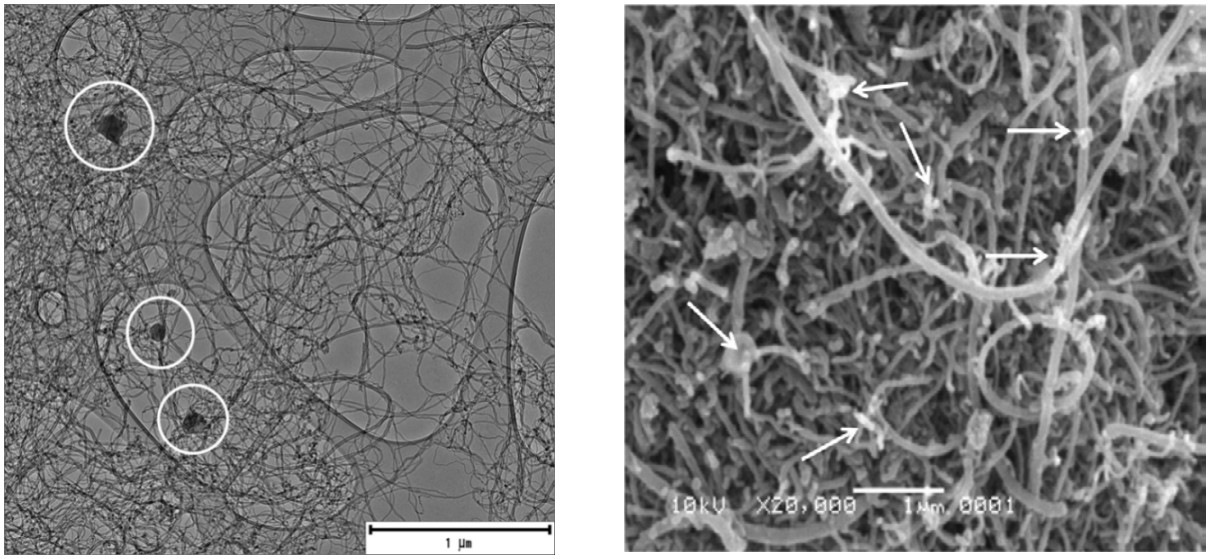

(a) (b)

Figure 4. 4 (a) TEM micrographs of the CNTs (b) A sample of TEM micrograph indicating lumpy material (Yudianti et al., 2011).

Similar material was identified on pristine CNTs in a study reported by Yudianti et al. (2011) as depicted in Figure 4.4 (b). The authors identified the lumpy material as particle impurities, usually in the form of graphitic, metal catalytic and amorphous carbon attached to the carbon fiber surface of CNTs during the synthesis process. The analysis and comparisons of the CNTs used in this work shows consistency to findings from previous work on characterisation of CNTs using TEM.

To examine the morphologies of the synthesized membranes, SEM analysis was carried out on the polysulfone membranes and the MMMs. SEM has been previously used to examine the morphology of a polyamide membrane infused with single walled CNTs in a study conducted by Barona et al. (2013). In addition, Maphutha et al. (2013) employed SEM as the characterization technique to study the morphology of polysulfone membranes infused with CNTs with a PVA layer. Hence, the use of the SEM micrographs assisted in confirming the presence of CNTs in the MMMs. In line with the aforementioned studies, the characterization of the CNTs and the prepared MMMs in this study was done using SEM.

The specimens of the polysulfone membranes were perpared for SEM analysis as described elsewhere (Han and Bhattacharyya, 1995), where membranes samples were fractured cryogenically using liquid nitrogen and dried at room temperature prior to coating with gold and palladium alloy. The preparation of the polysulfone membranes for SEM in this work entailed immersing the membrane samples in liquid nitrogen for five minutes and quick fracturing to expose the cross sectional area prior to mounting on the specimen holder. According to Liu et al. (2010), for SEM analysis, the sample should be conducting or semiconducting. However, since polymeric substances are non conducting coating is necessary.

The mounted membrane specimen were double-coated with a palladium and gold alloy as well as silver paint. Coating of the membranes with good conduting alloys was done to prevent charging of the membrane specimen, known as the movement of the specimen when exposed to electrons which tend to excite the membrane resulting distorted SEM micrographs during SEM analysis. The morphology of the polysulfone membrane was then charaterised using the (FEI

FIB/SEMNova 600 Nanolab) SEM machine. The polysulfone membrane SEM micrographs were taken from a cross sectional view at high and low magnification. This was done to determine the average thickness of the membrane and to also charaterise the morphology of the membrane. The thickness of the polysulfone membrane was measured using the SEM at a various magnifications as depicted in Figure 4.5.

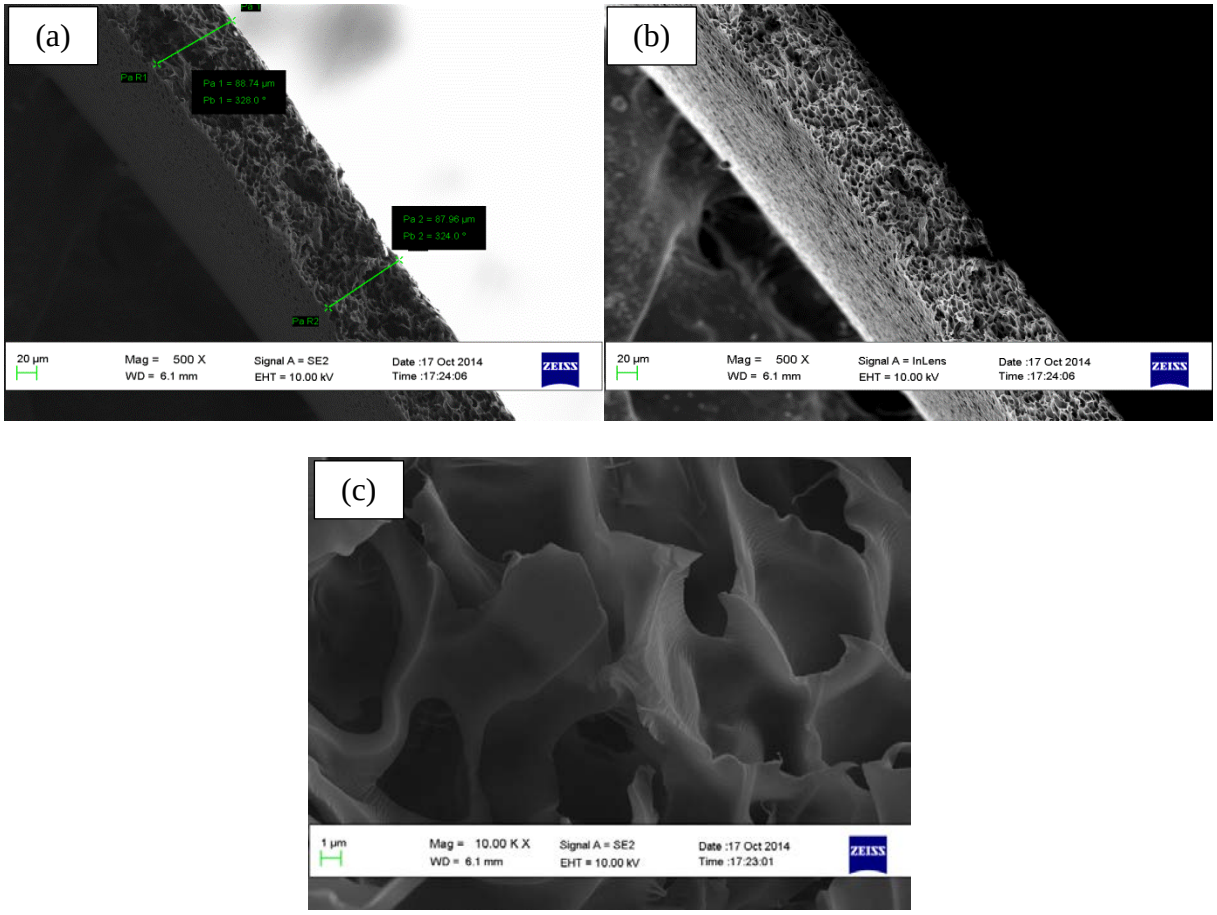

Figure 4. 5 **(a)** SEM micrographs of the cross-sectional view of the polysulfone membrane at high magnification (500 **X)**, showing the thickness of the polysulfone membrane; (b) SEM micrographs of the polysulfone membrane showing the porous cross-section, (c) indicating the polysulfone membrane surface morphology.

The thickness of the polysulfone membrane was measured to be between 88.74 μm and 87.96 μm, see Figure 4.5 (a), giving an average membrane thickness of 88.35 μm for the prepared polysulfone membrane. In previous studies by Han and Bhattacharyya (1995), it was shown that polymeric membranes prepared using the phase inversion method with DMF as a solvent and polysulfone as the precursor polymer resulted in membranes with porous cross sections and surfaces, attributable to rapid mass transfer between water and the solvent in a non-solvent bath. In this study, similar findings to that of Han and Bhattacharyya (1995) were obtained as polysulfone membranes with porous surface and cross sectional area were synthesized using the phase inversion method (see Figure 4.5 (b)).

According to Han and Bhattacharyya (1995), the preparation of membranes by the phase inversion method in a water bath resulted in a membrane surface with aggregates or nodules formed by liquid-liquid phase separation due to nucleation of the polymer-poor phase, whose aggregates were shown to contribute to the permeation characteristics of the membrane. The cross-sectional micrographs of the polysulfone membrane were taken at a magnification of 10 000X to evaluate the surface morphology of the polysulfone membrane, see Figure 4.5 (c). The SEM micrographs of the polysulfone membrane at a magnification of 10 000X, indicated finger-like protruding surface structures, see Figure 4.5 (c). Similar morphologies for pure polysulfone membranes were observed using SEM micrographs by Masuelli (2003) and Richards et al. (2012). Additional SEM micrographs of the polysulfone membranes are provided in Appendix B, Figure B1.

The specimens of the MMMs were prepared for SEM analysis similar to the analysis of polysulfone membranes. MMM samples were immersed individually in liquid nitrogen for five minutes and quickly fractured following removal from the liquid nitrogen to expose the cross sectional area prior to mounting on the specimen holder. Similar to the the preparation of the polysulfone membrane for SEM analysis, the MMMs samples were double coated with palladium and gold alloy and silver paint prior to mounting on the specimen holder to enhance the conductivity of the membranes in order to prevent charging during SEM analysis.

The morphology of the MMMs was then studied using the (FEI FIB/SEMNova 600 Nanolab) SEM machine. The MMMs SEM micrographs were taken from a cross-sectional view at high and low magnification to determine the average thickness of the membrane, and to confirm the presence of CNTs in the polymer matrix of the MMMs. The thickness of the polysulfone membrane was measured from the cross-sectional view of the MMM (see Figure 4.6).

The thickness of the M_1 MMM was measured to be between 62.33 μm and 68.95 μm, giving an average membrane thickness of 65.64 μm for the prepared MMM (see Figure 4.6). Similar to the polysulfone membrane, the M_1 MMM was prepared using the phase inversion method. The result from using this method showed that MMMs with a porous cross-sectional view and surfaces are obtained, which are similar to the previous findings of Maphutha et al. (2013). The images of the cross-sectional area of the M_1 MMM were taken at a magnification of 10 000X and the the surface morphology of the membrane confrimed the presence of CNTs in the polymer matrix, see Figure 4.6 (b) and Figure 4.6 (c).

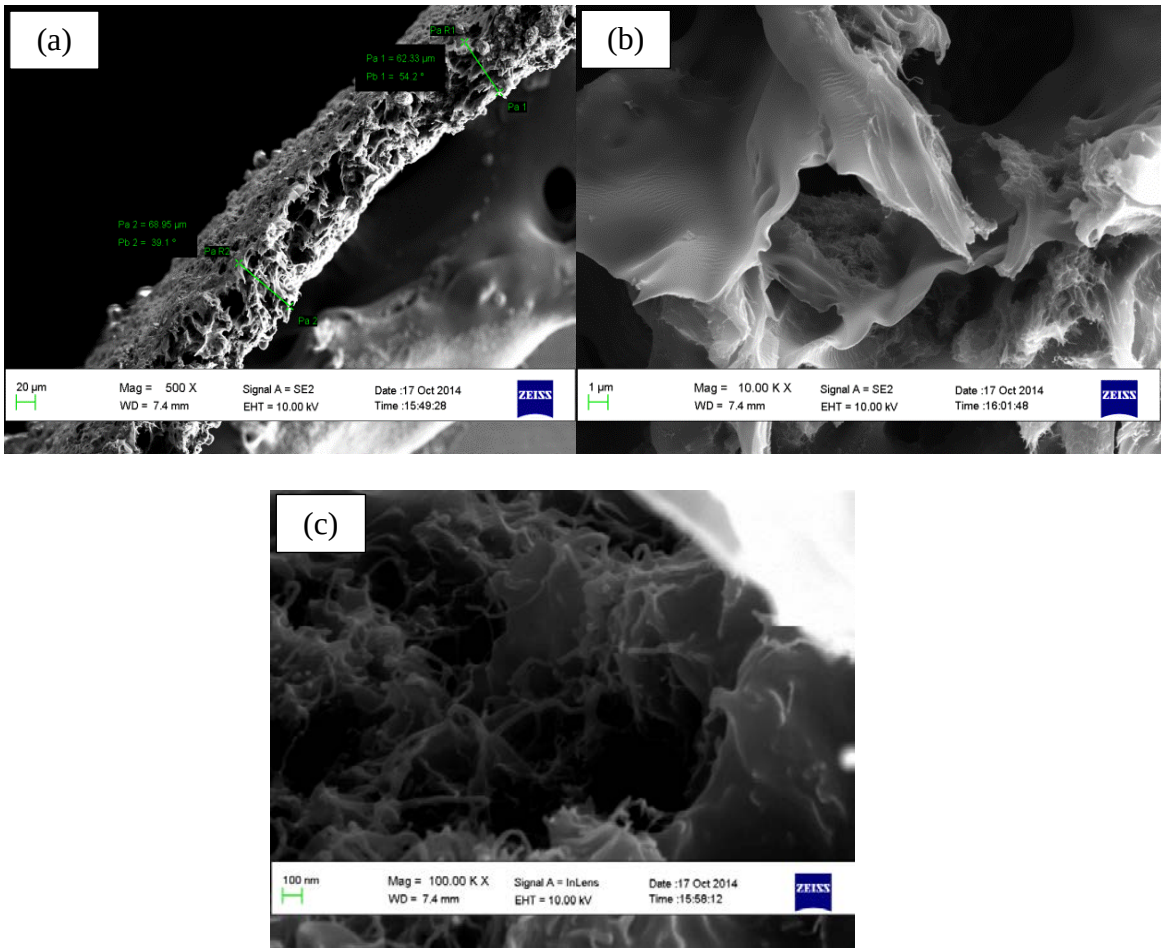

Figure 4. 6 SEM micrographs showing the cross-sectional view of the M_1 at high magnification (a) (500 **X**), (b) (10 000**X**) and (c) (100 000**X**) showing the surface morphology and the presence of CNTs in the MMM.

The SEM micrographs of the M_1 MMM at a magnification of 10 000X indicated a finger-like protruding surface structure similar to the prepared polysulfone membranes. However, the morphologies of the membranes are different because of the presence of CNTs in the polymer matrix, see Figure 4.6 (b). In order to further investigate the dispersion of the CNTs in the polymer matrix, SEM micrographs were taken at a magnification of 100 000X as depicted in Figure 4.6 (c).

The CNTs are shown to be integrated into the surface of the porous structure of the polysulfone matrix as revealed in Figure 4.6 (c). The entanglement of the CNTs, which was confirmed by the TEM micrographs of the CNT samples, is observed in the MMM cross section confirming the difficulty on homogeneous dispersion of the CNTs in a polymer matrix.

SEM analysis of M_2 was carried out similar to that of M_1, the thickness of the M_2 MMMs were measured from the cross-sectional view of the MMM using SEM micrographs (see Figure 4.7).

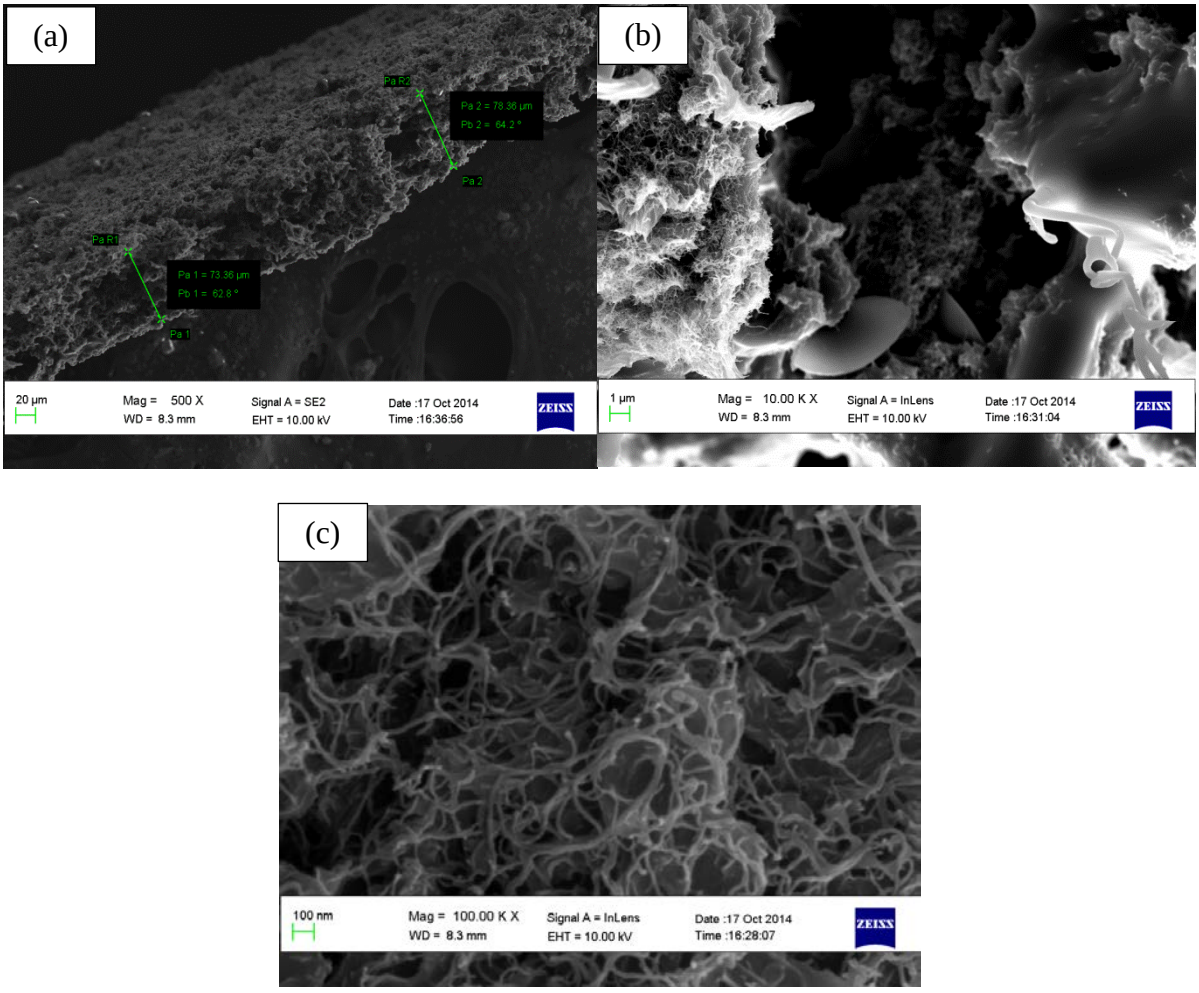

Figure 4. 7 SEM micrographs of the cross-sectional view of the M_2 at high magnification (a) (500 **X**), (b) (10 000**X**) and (c) (100 000**X**), showing the surface morphology and the presence of CNTs in the MMM.

Similar to observations made for M_1, the CNTs are shown to be mainly within the porous structure of the polysulfone matrix as revealed in Figure 4.7 (c).

Similar to M_1, the thickness of the M_3 MMMs were measured by examining the cross-sectional area of the membranes using the SEM micrographs (see Figure 4.8).

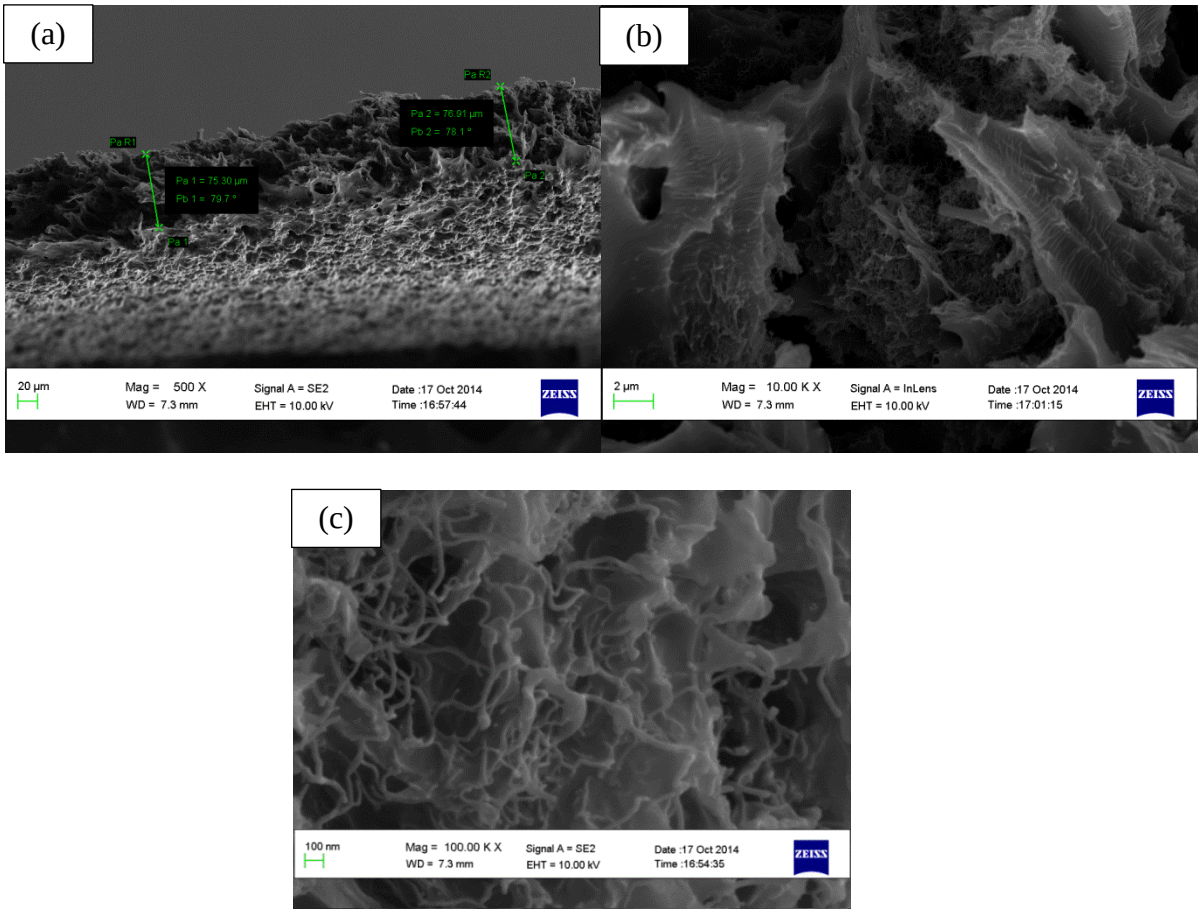

Figure 4. 8 SEM micrographs of the cross sectional view of the M_3 at high magnification (a) (500**X**), (b) (10 000**X**) and (c) (100 000**X**) showing the surface morphology and the presence of CNTs in the MMM.

The thickness of the M_3 was measured to be between 75.30 μm and 78.91 μm , see Figure 4.8 (a), giving an average membrane thickness of 77.11 μm for the prepared MMM. Similar to the M_4 membrane, M_1 and M_2, the M_3 were prepared using the phase inversion method. The result from using this method showed that MMMs with a porous cross-section and surfaces are obtained. The cross sectional view of the SEM micrographs of the M_3 MMM were taken at a magnification of 1 000X using the SEM machine. This was done to examine the surface morphology, see Figure 4.8 (c). The presence of CNTs in the polymer matrix is indicated by the fiber like structures on the surface of the polymer. In order to further evaluate the morphology of the CNTs in the polymer matrix, the SEM analysis was performed at a magnification of 100 000X as depicted in Figure 4.8 (c).

The M_3 MMM morphology observed indicates that the CNTs are integrated onto the surface of the porous structure of the polysulfone matrix which was observed for M_1 but not for M_2 MMMs. Similar to observations made for M_1 and M_2, the CNTs are shown to be entangled, which was confirmed by the TEM micrographs for the CNTs.

The comparison of the morphologies of the MMMs and the pure polysulfone membranes was done to study the main differences in the morphologies of the prepared MMMs compared to the polysulfone membrane. The morphology of the membranes revealed by the SEM micrographs in Figure 4.9 indicated that all membranes prepared have porous cross-sections and surfaces.

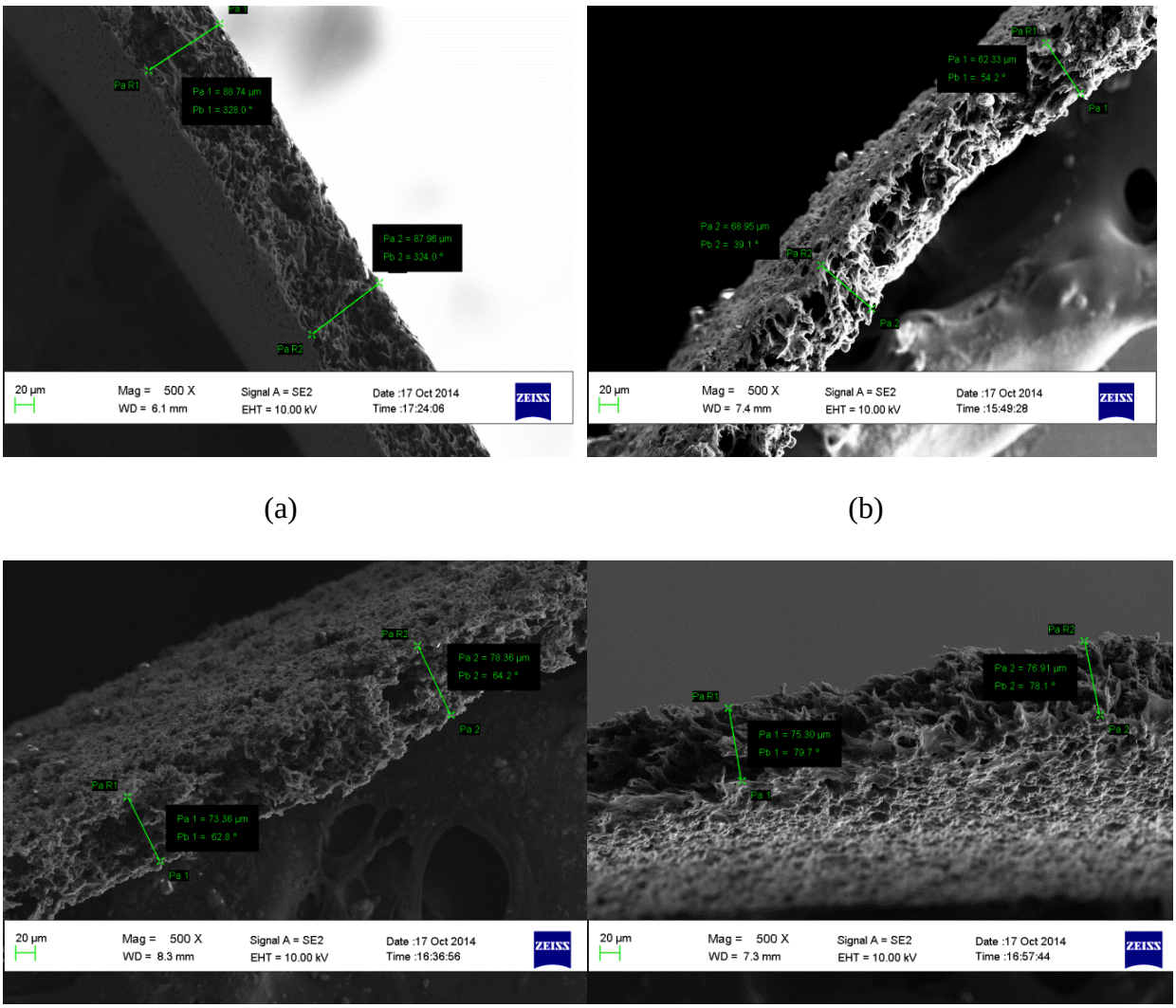

(a) (b)

(c) (d)

Figure 4. 9 SEM micrographs indicating the porous cross-section and surfaces of (a) M_1, (b) M_2, (c) M_3 and (d) M_4.

The membranes SEM micrographs were taken at magnification of 100 000X as depicted in Figure 4.10 to further examine the morphology of the porous surface.

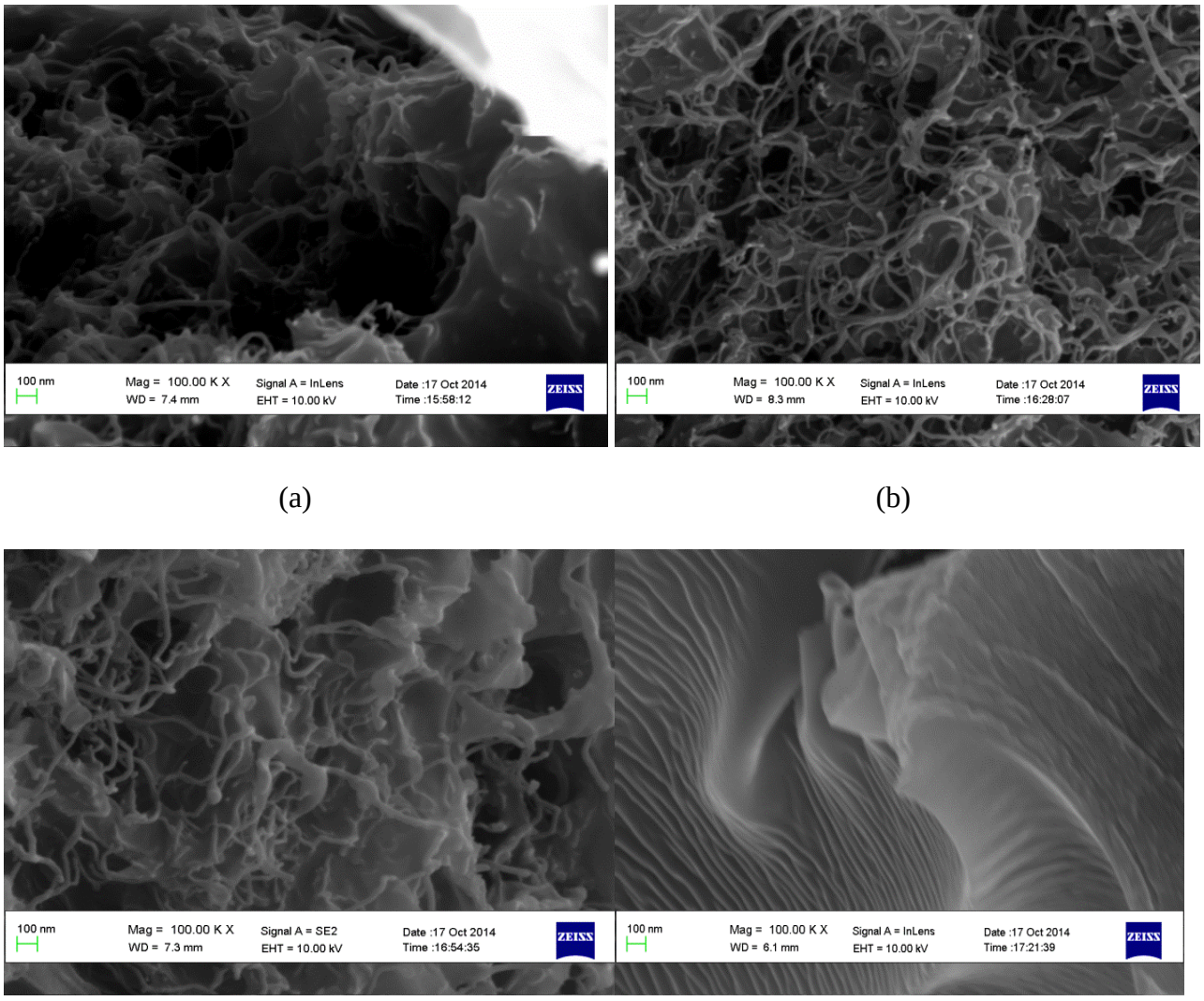

Figure 4. 10 SEM micrographs showing the cross-sectional area view of the membranes at high magnification for (a) M_1, (b) M_2, (c) M_3 and (d) M_4

In Figure 4.10, the presence of CNTs in M_1, M_2 and M_3 is shown whereas M_4 has a smooth clear finger like protruding structure. The morphologies of the MMMs are different as depicted in these images, confirming that the CNT dispersion methods used resulted in different CNT/polysulfone interfaces.

According to Yudianti et al. (2011), FTIR is used as qualitative technique for studying the functional groups on material. In a previous studies carried out by Voicu et al. (2011), which focused on the effect of the polymer coat improvement in the detection ability of sensing enzymes, FTIR analysis was used to determine the functional groups present on a CNT/polysulfone composite prepared using the phase inversion method. Voicu et al. (2011) showed that FTIR spectra can be used to verify the presence of CNTs in a polysulfone membrane infused with pristine and treated CNTs. In the study carried out by Alzahrani et al. (2013), the potential tertiary treatment of produced water using highly hydrophilic nanofiltration and reverse osmosis membranes, FTIR spectra was used to characterise the functional groups present on the membranes. Misra et al. (2007) used FTIR spectra in their study on FTIR spectroscopy of multi-walled carbon nanotubes to study nitrogen impurity attachments on CNTs. In the study reported by Masuelli (2003), FTIR was used to determine the functional groups present on polysulfone-acetylethanol ultrafiltration membranes prepared for application in oily wastewater treatment.

In this study, FTIR spectra were used to determine the functional groups present on surfaces of the polysulfone membranes, CNTs and MMM samples. The results obtained from the FTIR spectra for the CNTs, polysulfone membrane, M_4, and the M_1 MMM are depicted in Figure 4.11.

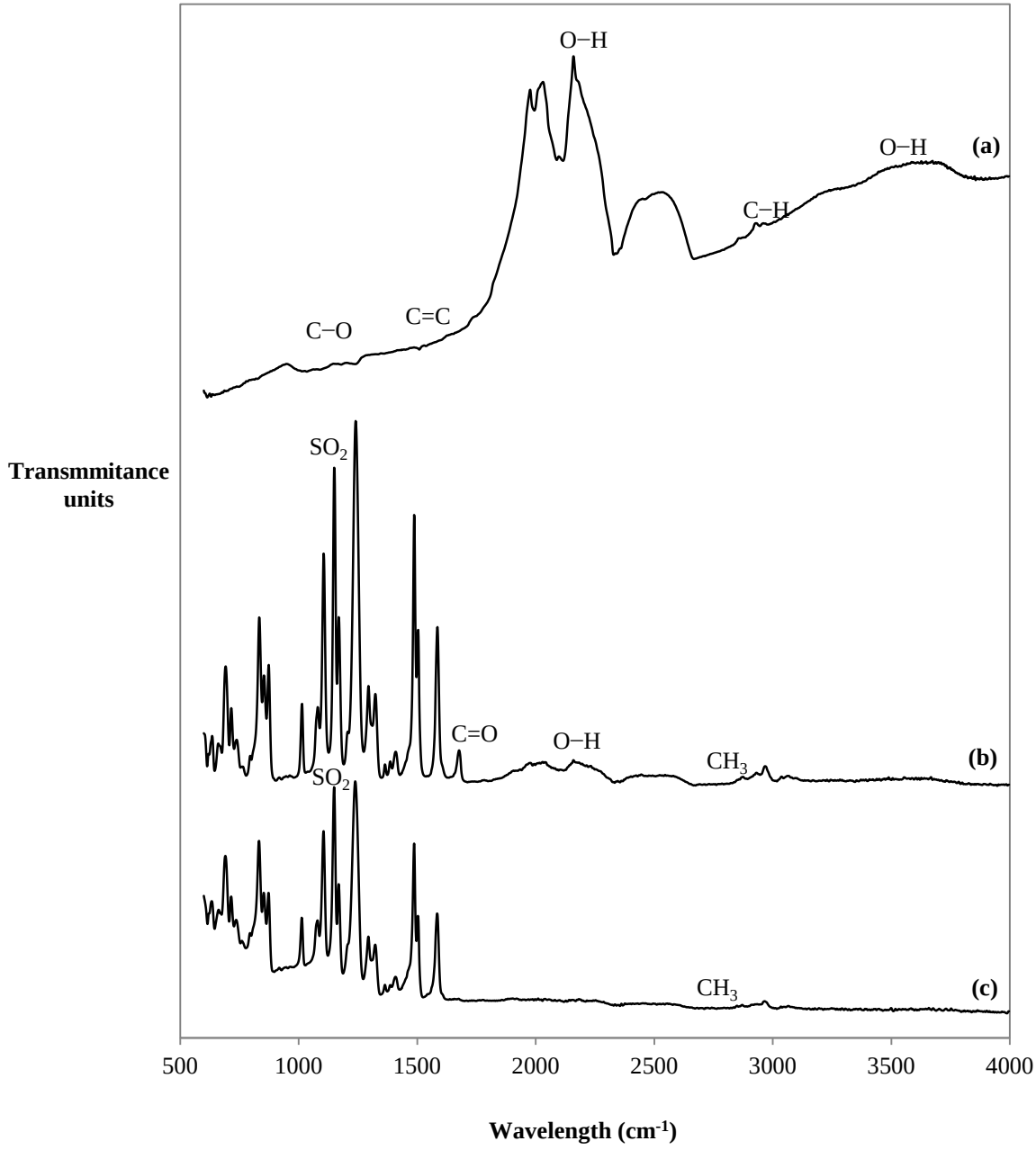

Figure 4. 11 FTIR spectra of (a) CNTs, (b) M_1 and (c) polysulfone membrane (M_4)

A peak at 1157 cm^{-1} was observed for the CNTs as depicted in Figure 4.11. Peaks in the region of 1100–1375 cm^{-1} have been attributed to esterified alcohol (C−O) groups by Pourfayaz et al. (2010), in their study of plasma functionalization of multi-walled CNTs (MWCNT) application in PMMA based nanocomposites using FTIR spectra. A peak of low intensity is observed at 1558 cm^{-1} for the CNTs, peaks ranging from 1532-1560 cm^{-1} have been attributed to C=C double bonding, which confirms the integrity of the hexagonal structure of pristine multi walled CNTs (Yudianti et al., 2011). Pourfayaz et al.(2010) reported that the C=C double bond is an indication of surface defects of CNTs which have been observed from the TEM micrographs of the CNT material depicted in Figure 4.3 thus validating this claim. Peaks at relatively high wavelengths, in the range above 3500 cm^{-1} to 3650 cm^{-1} were observed for the CNTs, which have been attributed to stretching vibrations of carboxylic groups according to the characteristic IR adsorptions of some functional groups (McCurry, 2008).

The most pronounced peaks for the CNTs were observed at wavelengths of 1971 cm^{-1}, 2165 cm^{-1} and 2923 cm^{-1} as depicted in Figure 4.11 (a). The pronounced peaks on the CNTs can be attributed to aromatic rings, carboxylic acid groups (O−H) and alkane groups (C−H) respectively, according to the characteristic IR adsorptions of some functional groups by McCurry (2008). Yudianti et al. (2011) observed functional groups including carboxylic acid (O−H), alkane groups (C−H), carbonyl compound groups (C=O) and carbon double bonds (C=C) in pristine and functionalised carbon nanotubes, confirming that functional groups observed for CNTs in this study is consistent with previous literature. Misra et al. (2007) reported that annealing of CNTs results in increased intensity of peaks following annealing in a Thermo-Gravimetric Analyser (TGA) at 400°C and 600°C. The FTIR spectra of the CNTs as

depicted in Figure 4.11 (a) suggest that some kind of treatment was carried out on the CNTs used in this study by the supplier. The dominant peaks for the polysulfone membrane, M_4, are mainly below the wavelength of 1500 cm^{-1} as depicted in Figure 4.11 (c). According to McCurry (2008), adsorption in this region is mainly due to a variety of single bond functional groups including alkane (C−C), alcohol (C−O) and amine (C−N) groups. The chemical structure of the polysulfone membrane is depicted in Figure 4.12.

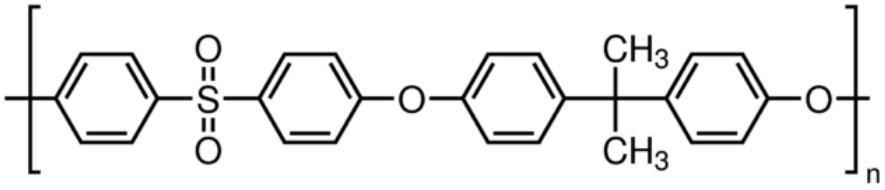

Figure 4. 12 Structure of the polysulfone polymer (Sigma Aldrich)

Figure 4.12 shows that the polysulfone structure is made up of Sulphur Dioxide (SO_2), aromatic rings and the Methyl (CH_3) groups. Peaks corresponding to the main functional groups (see Figure 4.11) which make up the polysulfone polymer structure were observed for M_4 at wavelengths of 1150 cm^{-1}, 2870 cm^{-1}, and 3210 cm^{-1}, which were attributed to the sulfur dioxide (SO_2) groups, the methyl (CH_3) groups, and the aromatic rings respectively.

The SO_2 functional group is observed at a wavelength of 1150 cm^{-1} and CH_3 at 2866 cm^{-1} which is consistent with findings of Voicu et al. (2011). A peak at 1587 cm^{-1} has been observed for the polysulfone membrane as depicted in Figure 4.11 (c), which falls in the 1450-1600 cm^{-1} range attributed to aromatic rings (McCurry, 2008). The FTIR spectra analysis of M_4 confirms the main structural components making up the polysulfone polymer. The effect of incorporating CNTs in the polymeric matrix for the prepared M_1 MMM on the functional groups was analysed, similar to the analysis done for the CNTs and the polysulfone membrane using the FTIR spectra. The dominant peaks for M_1, similar to the polysulfone membrane as depicted in Figures 4.11 (c) and (b), are mainly below wavelengths of 1500 cm^{-1} which have been attributed to single bond functional groups. Further analysis of the M_4 and M_1, indicates that the intensity of the peaks is more pronounced in the MMM when compared to the polysulfone membrane. Similar to M_4, M_1 was observed to have a peak at 1150 cm^{-1} and 1587 cm^{-1}, which have been attributed to the stretching vibrations of SO_2 and aromatic rings respectively shown to form part of the main structural components of the polysulfone polymer in Figure 4.12. The M_1 peaks observed below a wavelength of 1500 cm^{-1}, the SO_2 and aromatic rings peaks are intense compared to the peaks observed for the M_4.

A peak was observed at a wavelength of 1681 cm^{-1} for M_1 as depicted in Figure 4.11 (b), which was not a pronounced peak in the FTIR spectra analysis for the CNTs and polysulfone membrane depicted in Figure 4.11 (a) and (c). According to McCurry (2008), peaks ranging from 1670 cm^{-1} to 1780 cm^{-1} can be attributed to the carbonyl (C=O) functional group which was observed for the CNTs by Yudianti et al. (2011). Peaks for M_1 were observed at wavelengths of 1971 cm^{-1}, 2177 cm^{-1} and 2941 cm^{-1} as depicted in Figure 4.11 (b) similar to the CNTs as

depicted in Figure 4.11 (a). These peaks on the MMM have been attributed to aromatic rings, carboxylic acid groups (O−H) and alkane groups (C−H) respectively according to McCurry (2008). However, no peaks were observed for the polysulfone membrane at 1971 cm^{-1}, 2177 cm^{-1} and 2941 cm^{-1} indicating that the infusion of CNTs in the polysulfone matrix during MMM preparation influences the chemical properties of the resulting MMM, depending on the functional groups present on the CNTs.

Contact angle measurements of the synthesized pure polymer membranes and the MMMs were examined to characterize the membranes hydrophilic properties following the addition of nano particles during synthesis. Richards et al., (2012) measured the contact angle of deionized water on the membrane surface using the sessile drop method. Similar methods have been adapted in previous work by Jeong at al. (2007), Yu et al. (2013), Shawky et al. (2011) and Kim et al. (2012) to determine the hydrophilic properties of membranes. The contact angle tests of deionized water on the membranes surface were done to determine the hydrophilic properties of the MMMs relative to the polysulfone membrane as a result of addition of CNT particles into the polysulfone matrix during the preparation of the MMMs similar to previous studies using the sessile drop method. Ten deionized water droplets were placed on various locations of the membranes and the average results of the measured contact angle used as the contact angle for each of the membranes. The results are tabulated in Table 4.1.

Table 4. 1 Average contact angles measured using the sessile drop method.

Membrane	Contact angle (°)
M_1	76.6±5.0
M_2	77.9±1.3
M_3	77.3±4.5
M_4	88.1±2.1

M_4 has the highest measured contact angle compared to the MMMs, with a measured average contact angle of 88.1 ± 2.1° as shown in Table 4.1. M_2 contact angle was measured to be an average value of 77.9 ± 1.3°, with M_3 average contact angle was measured to be 77.9 ±1.3° and 76.6 ± 5.0° measured for M_1. The results obtained show that the addition of CNT in the polysulfone matrix results in a decrease in the contact angle as shown in Table 4.1. The CNT dispersion method adopted during the preparation of the MMMs have an influence on the contact angle of the resulting MMMs.

In previous studies, Richards et al. (2012) reported that a decrease in contact angle is an indication of improvement in the hydrophilic property of the membrane. Jeong at al. (2007), have also noted a decrease in the contact angle of polymeric membranes after the addition of fillers as an indication of an increase in the hydrophilic property of the membranes. The comparison between the contact angles of the membranes shows that M_1 is more hydrophilic amongst the membranes, as it has the lowest contact angle compared to the membranes prepared in this study, and M_4 is hydrophobic relative to MMMs as it has the highest contact angle as shown in Table 4.1. Masuelli (2003) calculated a contact angle of 77.9° for a polysulfone

membrane prepared using DMF and 2% Poly-Ethyl Glycol (PEG), which are similar to values obtained for the MMMs prepared in this study. The addition of PEG during synthesis appears to have contributed to the hydrophilic property of the membrane in their study as the values is lower compared to M_4, the polysulfone membrane in this study. In previous studies by Maphutha et al. (2013), a PVA layer was used to enhance the hydrophilic properties of the membranes in order to improve the anti-fouling property of the membrane. According to Yu et al. (2011), improved hydrophilicity is one of the fouling mitigating factors which implies that the MMMs prepared in this study are less likely to foul compared to the polysulfone membrane.

4.3.2 Evaluation of membrane performance

The pure water flux was determined by employing the Sterlitech cross flow filtration module from 1.38 bar to 6.9 bar, using Equation (4.1), in order to evaluate the initial performance of the membranes. The effective membrane area in the filtration cell was 42 cm^2. Water permeation flux readings were taken at room temperature after the membranes had been compacted for 4 hours at 8 bar. Deionized water was used for the initial permeation flux tests (see Figure 4.13).

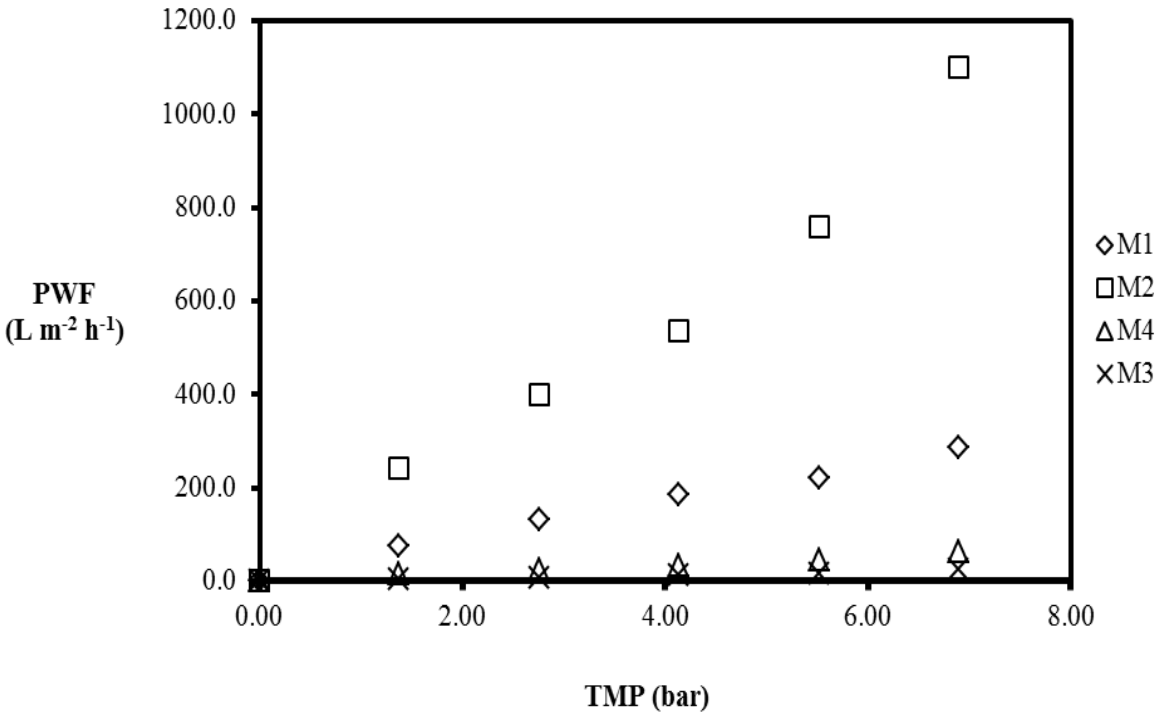

Figure 4. 13 Pure water flux of M_1, M_2, M_3 and M_4 from 1.38 bar to 6.9 bar.

The PWF at 6.9 bar was measured to be 287.7 $L.m^{-2} h^{-1}$, 1098.9 $L.m^{-2} h^{-1}$, 63.3 $L.m^{-2} h^{-1}$ and 25.2 $L.m^{-2} h^{-1}$ for M_1, M_2, M_3 and M_4 respectively. M_2 has the highest PWF for the given TMP range, followed by M_1 and M_3 which has the lowest PWF for the MMMs. Increasing the applied pressure enhanced the driving force for permeation, resulting in an increase in the permeation flux (Barona et al., 2013). Furthermore, the increase in the pure water flux for polymeric membranes has been attributed to the presence of hydrophilic sites on the filler particles as well as a low cross linking density (Barona et al., 2013).

The surface chemistry of the CNTs and MMMs were examined using FTIR spectra, confirming the presence of hydroxyl groups. Hence, it can be elucidated that the MMMs have a lower packing density compared to the pure polysulfone membranes. The incorporation of the CNTs in

the polysulfone matrix influences the pure water flux to varying degrees for the MMMs synthesized by adopting the three CNT dispersion methods. This has been confirmed by the PWF results obtained for the membranes.

Good membrane permeability has been listed as one of the requirements for good membrane technology. In this study the Pure Water Permeability (PWP) was defined as the ratio of the PWF and the TMP, the PWP results are depicted in Table 4.2.

Table 4. 2 The PWP results for M_1, M_2, M_3 and M_4 tested using de-ionized water at varying TMP.

		PWP ($L.m^{-2} h^{-1} bar^{-1}$)				
Membrane	**Contact angle (°)**	1.38 bar	2.76 bar	4.14 bar	5.52 bar	6.90 bar
M_1	76.6 ± 5.0	53.9	47.6	44.7	40.2	41.7
M_2	77.9 ± 1.3	174.5	183.2	145.0	137.3	159.3
M_3	88.1 ± 2.1	3.2	3.0	3.0	2.9	3.7
M_4	77.3 ± 4.5	11.1	8.5	8.3	8.1	9.2

The PWP at 6.9 bar was 41,7 $L.m^{-2} h^{-1} bar^{-1}$, 159.3 $L.m^{-2} h^{-1} bar^{-1}$, 3.7 $L.m^{-2} h^{-1} bar^{-1}$ and 9.2 $L.m^{-2} h^{-1} bar^{-1}$ for M_1, M_2, M_3 and M_4 respectively, see Table 4.2. M_2 has the highest PWP when

compared to M_1 and M_3 for the TMP range in this study, 1.38 bar to 6.9 bar. The highest PWF was calculated for this particular MMM (see Figure 4.13). M_3, has the lowest PWP relative to the MMMs and lowest PWF, indicating a direct relationship between the PWF and PWP. The incorporation of CNTs in the polysuflone matrix influences the permeability of the membranes as well as the pure water flux, suggesting that the CNTs play an active role on the performance of the MMMs. However, a 5% CNT loading was maintained for all the MMMs prepared using the three CNT dispersion methods during synthesis confirming that the CNT dispersion methods also impact the performance of the MMMs. The inconsistency in the results obtained for the PWF and PWP confirms the importance of the CNT dispersion during MMM synthesis.

Homogenous dispersion of MWCNTs in the polymer matrix has been reported to influence the interfacial interactions between the filler material and the polymer, ultimately affecting the performance of MMMs (Abdolmaleki et al., 2013). It can be elucidated that the presence of voids between the CNTs and the polysulfone in the MMMs, as a result of interfacial defects formed during synthesis adopting the three dispersion methods, affects the permeation flux and the permeability. Interfacial defects arising as a result of interface voids or rigidified polymer layers around the filler particles have been reported to influence the permeability of MMMs by Aroon et al. (2013). Furthermore, it be explained that M_3 has the least interfacial voids as well as the highest cross link density compared to the MMMs prepared using CNT dispersion method 1 and 2 because of the relatively low pure water flux obtained.

The separation of the oil-water mixture was carried out using the Sterlitech cross flow filtration module and the Oil-Water Flux (OWF) was measured for TMP from 1.38 bar to 6.90 bar, using Equation (4.1.) The effective membrane area was 42 cm^2. The OWF was measured at room

temperature after the membranes were compacted using an oil-water mixture at 8 bar for 4 hours. The emulsified oil and water solution, with an oil concentration of 1000 mg diesel/l water, was prepared by mixing water and diesel using a high speed stirrer for 4 hours. The initial concentration of oil is typical of as produced water from oil and gas reservoirs (Chakrabarty et al., 2008). The OWF as a function of the TMP is depicted in Figure 4.14.

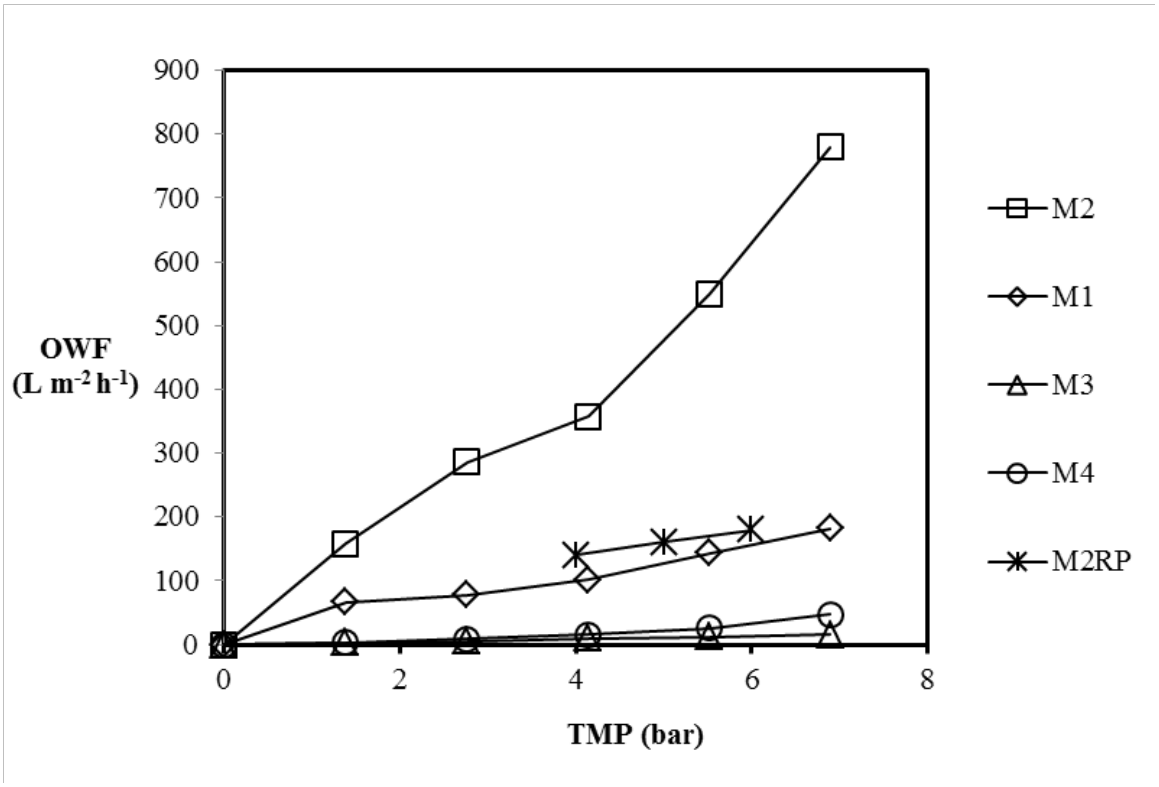

Figure 4.14 OWF of the membranes.

The OWF at 6.9 bar was measured to be 182.4 $L.m^{-2} h^{-1}$, 779.2 $L.m^{-2} h^{-1}$, 15.6 $L.m^{-2} h^{-1}$ and 47.6 $L.m^{-2} h^{-1}$ for M_1, M_2, M_3 and M_4 respectively. M_2 displayed the highest OWF for the given TMP range and the PWF for this MMM was the highest recorded for all the MMMs. However, the OWF is lower than the PWF obtained for M_2 for the given TMP range. M_1 has the second

highest OWF after M_2 and M_3 has the lowest OWF at 6.9 bar for the MMMs (see Figure 4.14). M_4 was observed to have a higher OWF than M_3 while the PWF for M_4 was higher than that of M_3 at 6.9 bar. The performance results of CNT/polysulfone MMMs with a PVA layer prepared by Maphutha et al. (2013) have been included in this study for comparison, the notation used for this MMM was M_{2RP}. The CNT dispersion method adopted in preparing the M_{2RP} MMMs was reported as CNT dispersion Method 2 (Maphutha et al., 2013).

The polysulfone membrane, M_4, has the lowest OWF in comparison to M_1, M_2 and M_{2RP}. However, this MMM has higher OWF relative to M_3 as depicted in Figure 4.14. Maphutha et al. (2013) reported that the OWF for CNT/polysulfone MMMs is higher than that of the pure polysulfone membranes which is in agreement with the results obtained for M_1 and M_2. However, the OWF calculated for M_3 is not consistent with their finding, which further confirms that the CNT dispersion method adopted during synthesis affects the performance of the MMMs.

The observation made for PWF and the OWF for M_4, is that the pure water permeation flux is lower compared to that of the oil-water mixture for the TMP range, 1.38 bar to 6.90 bar. The increase in the permeation flux from pure water to the oil-water mixture for the polysulfone membrane, M_4, can be attributed to hydrophobic nature of the membrane. The contact angle was measured to be 88.1 ± 2.1^{o}, and the presence of Methyl groups was confirmed using the FTIR spectra. Methyl groups were reported to be responsible for hydrophobic properties by Husain and Koros (2007).

The OWF for M_{2RP} is considerably lower compared to that calculated for M_2 (see Figure 4.14). The PVA layer added on the M_{2RP} was reported to enhance the hydrophilic properties (Maphutha et al., 2013). However, from observation and comparison to the M_2 MMM, the PVA layer can potentially reduce the permeability of the MMMs. The Oily Water Permeability (OWP) was calculated using Equation (4.2) and the results are summarized in Table 4.3.

Table 4. 3 OWP for M_1, M_2, M_3 and M_4, M_{2PR} using de-ionized water.

	OWP (L m^{-2} h^{-1} bar^{-1})								**Refer**
	1.38 bar	2.76 bar	4.00 bar	4.14 bar	5.00 bar	5.52 bar	6.00 bar	6.90 bar	
M_1	47.8	28.2	-	24.7	-	26.0	-	26.4	This study
M_2	114.4	103.6	-	86.3	-	137.3	-	113.0	This study
M_{2RP}	NR	NR	32.5	NR	32.0	NR	30.0	NR	Maphutha et al. (2013)
M_3	2.5	2.0	-	2.3	-	2.2	-	2.3	This study
M_4	1.9	3.0	-	3.7	-	4.7	-	6.9	This study

**NR means the values could not be calculated as the data required was not reported*

The OWP at 6.9 bar was 26.4 $L.m^{-2}\,h^{-1}\,bar^{-1}$, 113.0 $L.m^{-2}\,h^{-1}\,bar^{-1}$, 2.3 $L.m^{-2}\,h^{-1}\,bar^{-1}$ and 6.9 $L.m^{-2}\,h^{-1}\,bar^{-1}$ for M_1, M_2, M_3 and M_4 respectively as depicted in Table 4.3. The PWP at 6.9 bar was 41,7 $L.m^{-2}\,h^{-1}\,bar^{-1}$, 159.3 $L.m^{-2}\,h^{-1}\,bar^{-1}$, 3.7 $L.m^{-2}\,h^{-1}\,bar^{-1}$ and 9.2 $L.m^{-2}\,h^{-1}\,bar^{-1}$ for M_1, M_2, M_3 and M_4 respectively (see Table 4.2), confirming an decrease in the permeability of the MMMs from pure water compared to oil-water mixtures. However, the OWP was higher than the PWF (see Table 4.2 and Table 4.3).

The OWP for M_2 is higher than the OWP for M_1, M_{2RP}, and M_3 (see Table 4.3). M_3 has the lowest OWP of all the MMMs prepared in this study and the OWP of M_4, is greater than that of M_3 (see Table 4.3). Disparities are observed in the performance of the MMMs prepared using the three CNT dispersion methods and are confirmed by the MMM performance.

The OWP for M_{2RP}, calculated using the reported OWF and TMP by Maphutha et al. (2013), is lower than that of the M_2 MMM prepared in this study although these MMMs were synthesized using CNT dispersion method 2. Porous filler blockage has been reported to significantly reduce the performance of MMMs (Aroon et al., 2010). This can be attributed to the reduced OWP of M_{2RP} as a result of the PVA layer addition to the MMM during synthesis.

In order to further evaluate the performance of membranes, the oil rejection was calculated using Equation (4.4.). Samples of oil-water permeate were taken during separation and a composite sample prepared for analysis, representing the overall performance of each of the membranes. The UV spectrophotometer was used for the water analysis. The oil rejection results for the membranes are depicted in Figure 4.15.

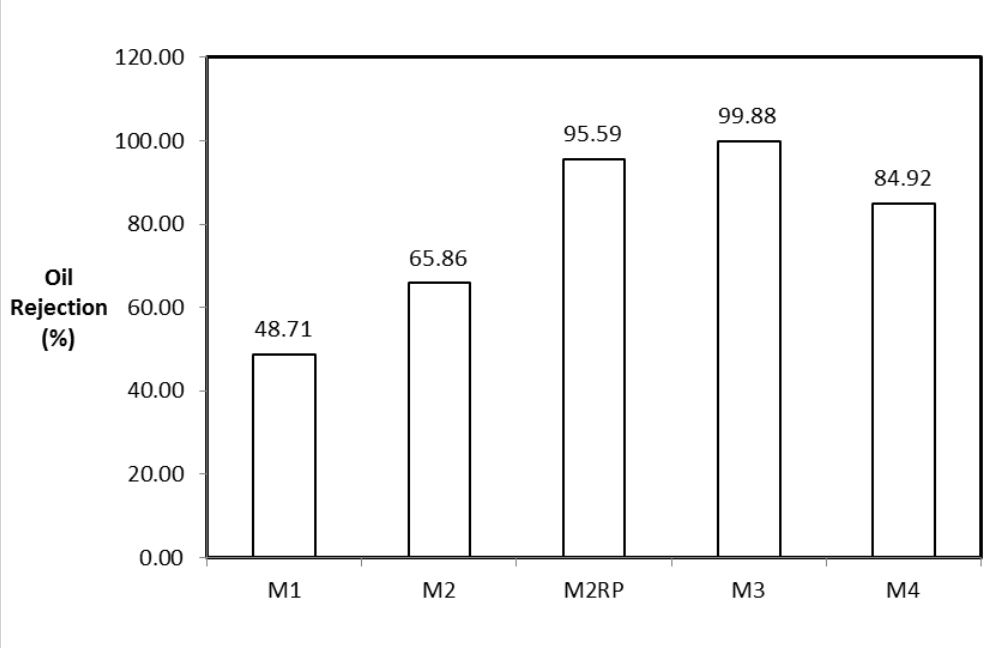

Figure 4.15 The oil rejection for the membranes.

The highest oil rejection achieved in this study was 99.88% for M_3 as depicted in Figure 4.15. M_3 displayed the lowest PWF, PWP, OWF as well as OWP. M_4 oil rejection was calculated to be 84.92%, which is higher than the oil rejection obtained for M_1 and M_2 (M_1= 48.71% and M_2 = 65.86%). The rejection reported by Maphutha et al. (2013) for M_{2RP} was 95.59%. The selectivity of the membranes, in particular M_3, has been shown to be higher compared to that of M_4, suggesting that dispersion of CNTs in M_3 is better compared to that of M_1 and M_2. The surface chemistry of the CNTs has been shown to be hydrophilic (see section 4.3.1), with the presence of hydroxyl groups, which suggests that MMMs with uniformly dispersed hydrophilic CNTs in the polymer matrix could have a higher affinity for water as opposed to oil.

The oil which was used in this study was diesel, with components generally from the C_8 to C_{21} alkane groups. The kinetic diameter of C_8 is 7.5Å (0.75 nm) (Gallagher and Brown, 2008) and the kinetic diameter of water has been reported as 2.6 Å (0.26 nm) by Jae et al. (2011). The kinetic diameter of hydrocarbons have been shown to increase with increasing carbon numbers (Shao and Huang, 2006), suggesting that the components in diesel will have bigger kinetic diameters than that of C_8. The competition between water and oil to occupy the porous sites of the membranes is clearly shown by the low rejection on M_4, indicating that the surface chemistry of the polysulfone membranes favor the absorption of oil over water. The low rejection observed for M_1 and M_2 is attributed to poor CNT dispersion and formation of interfacial defects between the CNT and polymer matrix, resulting in free fraction volume that enhanced the permeation flux as well as the permeability.

4.4 Summary

The CNT/polysulfone MMMs with 5% MWCNT loading and pure polysulfone membranes were synthesized using the phase inversion method. Three CNT dispersion methods were adopted during the synthesis of the MMMs. The membrane and CNT characterisation was conducted to study the morphology, the surface chemistry as well as the hydrophilic properties. SEM micrographs revealed porous cross sections and surface morphologies of the MMMs and polysulfone membranes. However the degree of CNT dispersion within the polysulfone matrix was less pronounced for the MMMs prepared using CNT dispersion method 2. The functional groups observed for the MMMs and CNTs using FTIR spectra included carboxylic acid groups (O−H), carbonyl groups (C=O), and oxygen containing groups, which have been reported to be responsible for the hydrophilic properties. The contact angles measured for the MMMs using CNT dispersion methods 1, 2 and 3 were 76.6 ± 5.0°, 77.9 ± 1.3°, and 77.3 ± 4.5° respectively,

while 88.1±2.1° was measured for the pure polysulfone membranes. The oil rejection obtained for MMMs synthesized by adopting CNT dispersion method 1, 2 and 3 was 48.71%, 65.86% and 99.88% respectively. The pure polysulfone membranes oil rejection was 84.92%. The pure water and oil water flux increased with increasing trans-membrane pressure for all the membranes. The oily water permeability of the MMMs was 26.4 L m^{-2} h^{-1} bar^{-1}, 113 L m^{-2} h^{-1} bar^{-1} and 2.3 L m^{-2} h^{-1} bar^{-1} for MMMs prepared using CNT dispersion method 1, 2 and 3 respectively, and the pure polysulfone membrane oily water permeability was 6.9 L m^{-2} h^{-1} bar^{-1} at 6.9 bar.

The competition between water and oil to occupy the porous sites of the membranes was confirmed by the low oil rejection result for M_4, indicating that the surface chemistry of the membranes favored the absorption of oil over water. The low rejection observed for M_1 and M_2 was attributed to poor CNT dispersion and formation of interfacial defects between the CNT and polymer matrix, resulting in free fraction volume that enhanced the permeation flux as well as the permeability. The adoption of CNT dispersion Method 3 produced MMMs with exceptional oil rejection as well as good permeability.

Chapter Five

Effect of particle size of CNTs on the performance of CNT/Polysulfone composite membranes

5 Effect of particle size of CNTs on the performance of CNT/Polysulfone composite membranes

5.1 Introduction

Chapter 4 of this study focused on determining the best CNT dispersion method to adopt during the preparation of MMMs. It has been shown that in terms of oil rejection, membranes prepared using dispersion method 3 displayed the best performance during the separation of oil-water mixture. Oil rejection of M_3 was shown to be 15% higher than that of the pure polysulfone membrane and 4.25% higher than that of the membrane previously reported (Maphutha et al., 2013).

This chapter focuses on evaluating the effect of CNT particle size on the performance of membranes prepared using CNT dispersion method 3 during the separation of oil-water mixture. The materials used, the methods adopted in preparing the membranes, the results and discussion as well as a summary of the findings are described.

5.2 Experimental

5.2.1 Materials

Polysulfone, DMF and two CNT samples with varying particle sizes were purchased from Sigma Aldrich. The polysulfone polymer supplied was in beaded form with molecular weight specified to be 22 000 g/mol and DMF with molecular weight specified as 73.09 g/mol. CNTs used in chapter 4 of this study were specified by the supplier with OD 6-9 nm x length 5 μm and carbon basis greater than 90%. The CNTs added as part of the study for evaluating the effect of CNTs

particle size on the performance of MMM were specified as having diameters ranging from 110-170 nm x length 5-9 μm. The latter CNT material has been referred to in this report as CNT II and the carbon nanotubes used in Chapter 4 of this study have been referred to as CNT I in order to be able to differentiate the two samples.

5.2.2 Methods

MMMs were prepared by adopting CNT dispersion method three as reported in Chapter 3 with CNT loading of 5% which was the CNT loading similar to loading used in Chapter 4. The MMMs were prepared using CNT dispersion method 3 via the phase inversion method. The MMMs prepared using CNT II samples were referred to as M_5. The same convention was maintained for MMMs prepared using CNT I samples similar to Chapter 4, these MMMS have been referred to as M_5. The CNT were characterized using TEM similar to previous studies by Kim et al. (2012), Yin, Zhu and Deng (2013) in order to evaluate the CNT size and morphology. FTIR was used to evaluate and compare the functional groups for both CNT samples used in this study, similar to previous work by Misra et al. (2007), Yudianti et al. (2011) and Zhao et al. (2014). The MMMs were characterized using FTIR to evaluate and compare the influence of the two CNT samples on the functional groups of the MMMs, similar to previous studies (Richards et al., (2012), Barona et al. (2013) and Masuelli (2013)). The contact angle of the MMMs was evaluated using the sessile drop method using deionized water, similar to previous work by Jeong et al. (2007), Yu et al (2011), Shawky et al. (2011) and Alzahrani (2013) in order to quantify the hydrophilicity of the membranes. The performance of the MMMs was evaluated using the Sterlitech cross flow module as described in chapter 3. The overall process flow for evaluating the effect of CNT particle size on CNT/polysulfone MMMs is depicted in Figure 5.1.

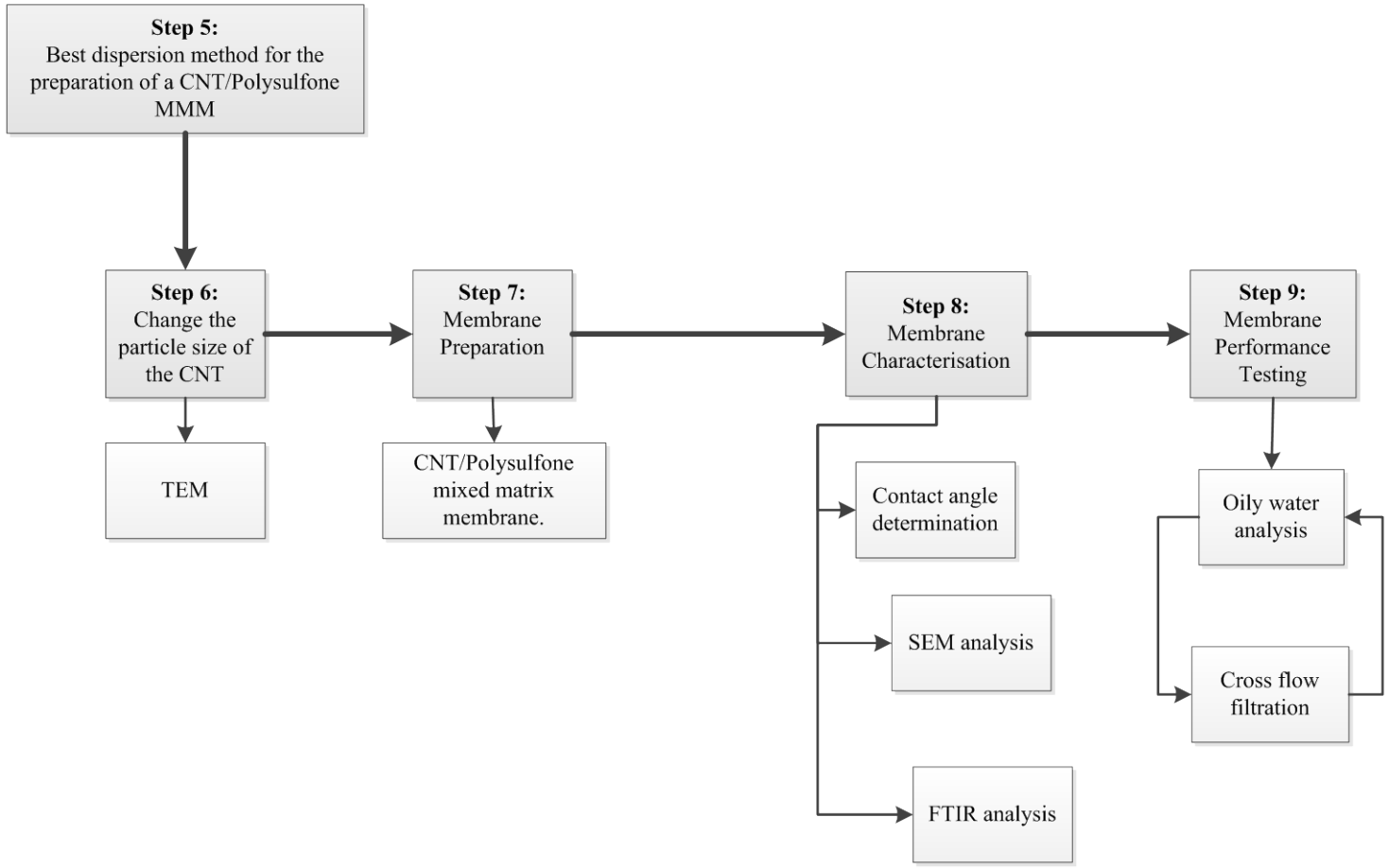

Figure 5. 1 Overall flow diagram for membrane preparation, characterisation, performance evaluation and testing to be employed in evaluating the effect of CNT particle size on MMM performance during oil and water separation.

5.3 Results and Discussion

5.3.1 Physico-chemical characterization of CNT and synthesized membranes

The CNT samples were examined using the FEI Technai TEM operated at a voltage of 120 kV in a similar manner to Chapter 4. The TEM micrographs of CNT I and CNT II samples are depicted in Figure 5.2.

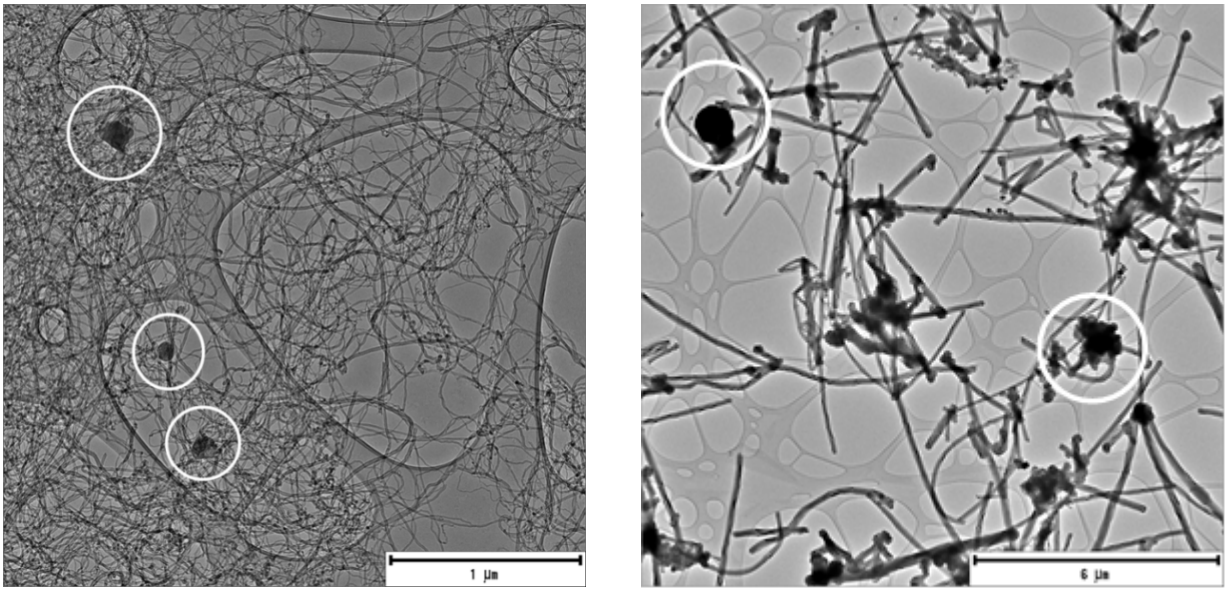

(a) (b)

Figure 5. 2 TEM micrographs of the CNT samples showing (a) CNT I (b) CNT II

Comparing the CNTs, the TEM micrograph for CNT I indicates the entanglement of the nanotubes whereas less entanglement is observed in CNT II samples as depicted in Figure 5.2

which can be attributed to the difference in length of the CNT samples. Further analysis of the CNTs TEM micrographs indicates lumpy material adhering to the CNTs surface for both CNT I and CNT II samples. This has been attributed to particle impurities, usually in the form of graphitic, metal catalytic and amorphous carbon, attached to the carbon fiber surface of CNTs during the CNT synthesis process (Yudianti et al., 2011). The prevalence of the impurities is much higher for CNT II samples compared to CNT I. The surface morphology of the CNTs is depicted in Figure 5.3

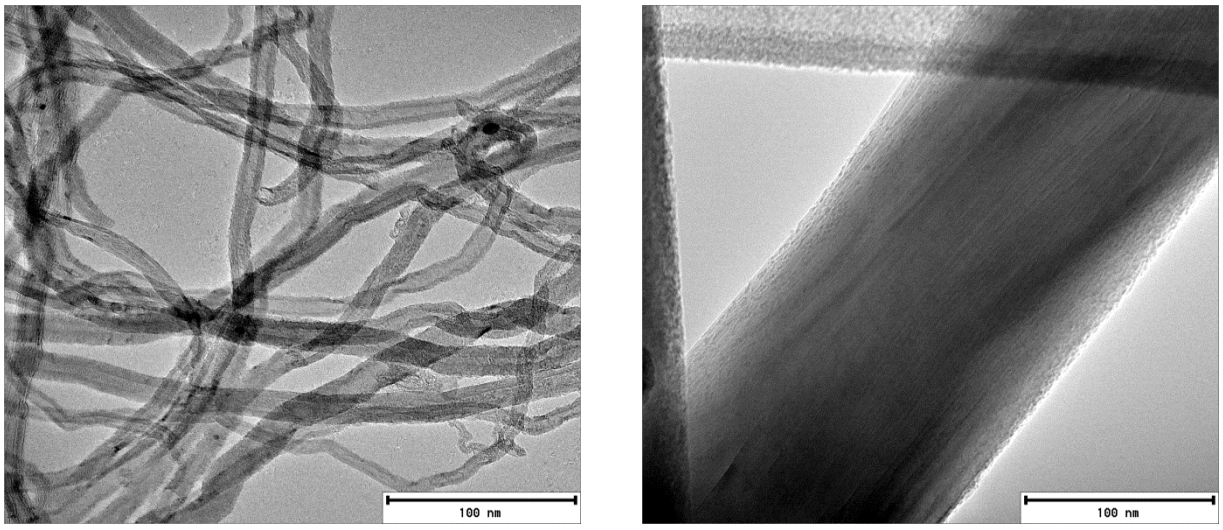

(a) (b)

Figure 5. 3 TEM micrographs of (a) CNT I and (b) CNT II

Surface defects are observed for CNT I samples as depicted in Figure 5.3 (a). However, none are observed for CNT II samples. Carbon layers forming were observed for both CNT I materials confirming that the CNTs are multi-walled. Some close ended tubes were observed for CNT I and not for CNT II material (see Figure 5.3).

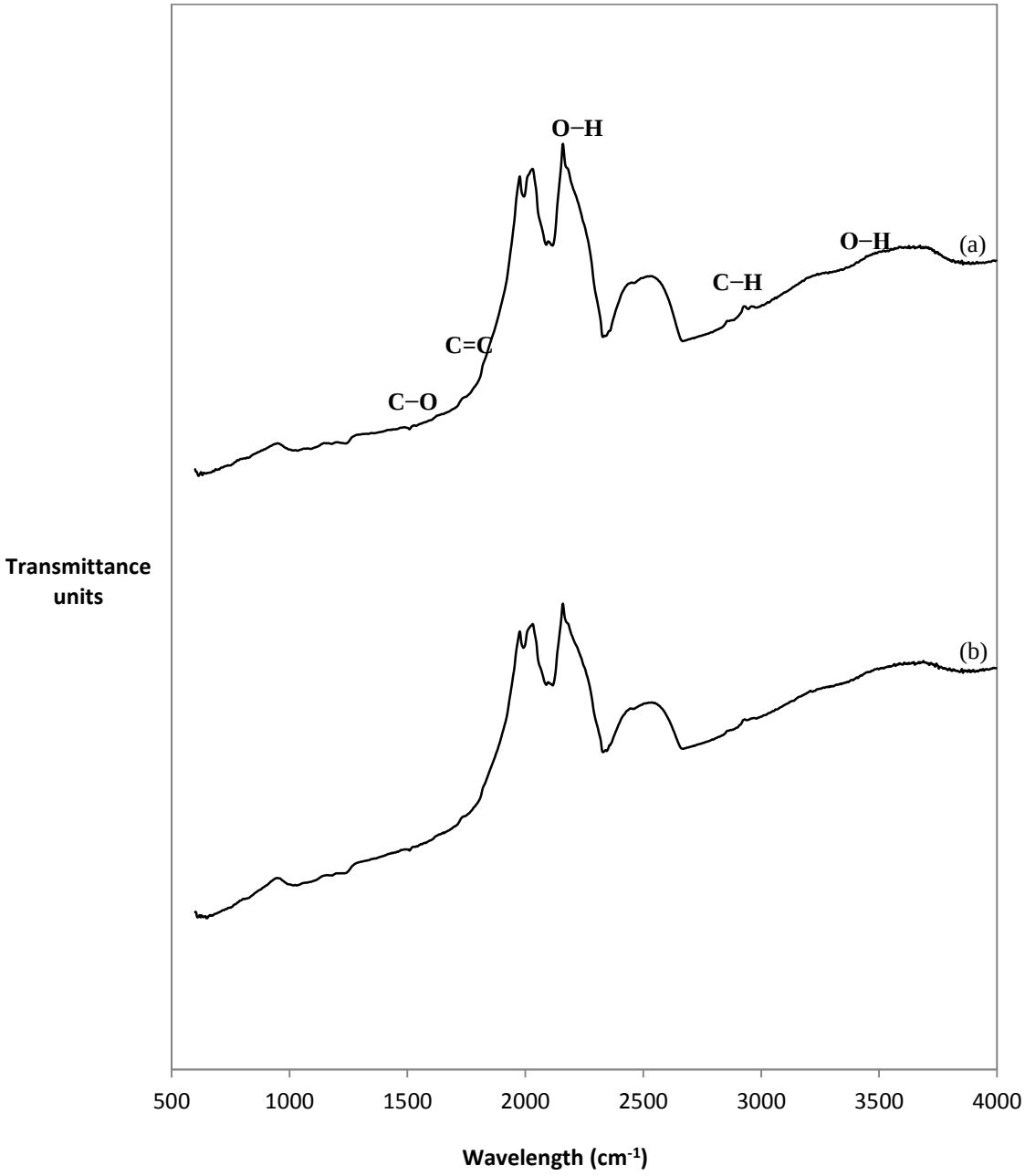

Figure 5.4 FTIR spectra analysis of (a) CNT I and (b) CNT II samples.

Similar FTIR spectra profiles are observed for both CNT I and CNT II samples as depicted in Figure 5.4. This is an indication that the inherent chemical composition and functional groups of both the CNTs samples used in this study was similar. In Chapter 4 of this study, it was shown that the functional groups present in the CNT I samples included aromatic rings, carboxylic acid groups (O−H) and alkane groups (C−H). Examining the FTIR spectra for both CNT I and CNT II samples, peaks at 1157 cm^{-1} were observed as depicted in Figure 5.4 (a) and (b) respectively. Absorbance peaks ranging from 1100–1375 cm^{-1} have been attributed to esterified alcohol (C−O) groups by Pourfayaz et al. (2010) in their study of plasma functionalization of multi walled CNTs using FTIR spectra, elucidating to the presence of alcohol groups in the structure of both the CNT samples.

Peaks of low intensity were observed at 1558 cm^{-1} for both CNT I and II. Peaks ranging from 1532-1560 cm^{-1} have been attributed to C=C double bonding, which confirms the integrity of the hexagonal structure of pristine multi walled CNTs (Yudianti et al., 2011). In the study by Pourfayaz et al. (2010), the C=C double bond were reported to be an indication of surface defects of CNTs. Comparison of the C=C for both CNT samples show that the absorbance intensity is very low, which can be an indication of minimal surface defects, confirmed on the TEM analysis of the CNTs. Peaks at relatively high wavelengths, in the range above 3500 to 3650 cm^{-1}, were observed for both CNT I and CNT II, which have been attributed to stretching vibrations of carboxylic groups according to characteristic IR adsorptions of some functional groups (McCurry,2008).

The most pronounced peak for both the CNTs were observed at wavelengths of 1971 cm^{-1}, 2165 $cm^{-1}$and 2923 cm^{-1} as depicted in Figure 5.4 (a) and (b). The pronounced peaks on the CNTs can be attributed to aromatic rings, carboxylic acid groups (O−H) and alkane groups (C−H) respectively according to the characteristic IR adsorptions of some functional groups (McCurry, 2008).

Yudianti et al. (2011) observed functional groups including carboxylic acid (O−H), C−H, alkane groups (C−H), carbonyl compound groups (C=O) and carbon double bonds (C=C) in pristine and functionalised carbon nanotubes, confirming that functional groups observed for the CNTs in this study is consistent with literature. Misra et al. (2007) reported that annealing CNTs results in increased intensity of peaks following annealing the CNTs in a Thermo-Gravimetric Analyser (TGA) at 400°C and 600°C, from observing the FTIR spectra of the CNTs as depicted in Figure 4.11 (a) it can be inferred that some kind of treatment was done on both CNTs by the supplier.
Similar to the procedure detailed in Chapter 4, contact angle tests were conducted to determine the hydrophilic properties of the MMMs as a result of addition of CNT particles. The results are shown in Table 5.1.

Table 5. 1 Measured average contact angles of the membranes.

Membrane	**Contact angle (°)**
M_3	77.3 ± 4.5
M_5	78.8 ± 5.6

The contact angle of M_3 is 77.3 ± 4.5° and that of the M_5 is 78.8 ± 5.6° (see Table 5.1). As previously discussed, a relatively low contact angle is an indication of the enhanced hydrophilic property of the membrane. M_3 and M_5 membranes are both hydrophilic compared to the polysulfone membrane, M_4, which has a measured contact angle of 88.1 ± 2.1°.The addition of CNTs in the polymer matrix enhances the hydrophilic property of the membrane, which in turn influences the surface chemistry of the filler material. The functional groups observed for the CNT samples used during the synthesis of both M_3 and M_5 were similar, as shown by the FTIR spectra, as well as the dispersion method used during the preparation of these MMMs. This implies that the particle size of the CNT also influences hydrophilic property of the MMMs when infused in a polysulfone matrix. The difference in the average contact angle measured for M_3 and M_5 is 1.5° which is not very significant. However, since the contact angle has been used to determine the fouling tendencies of membranes (Aroon et al., 2013), the M_3 is likely to have improved fouling tendencies when compared to M_5. The TEM micrographs of the CNT samples used during the preparation of the MMMs in this section shows that the CNT used for M_3 were entangled, with similar observations from the SEM micrographs in 4.3.1, implying that more hydrophilic sites were present in M_3 than M_5.

5.3.2 Evaluation of Membrane Performance

The membrane performance was evaluated as described in 4.3.2. The pure water flux results for the MMMs are depicted in Figure 5.5.

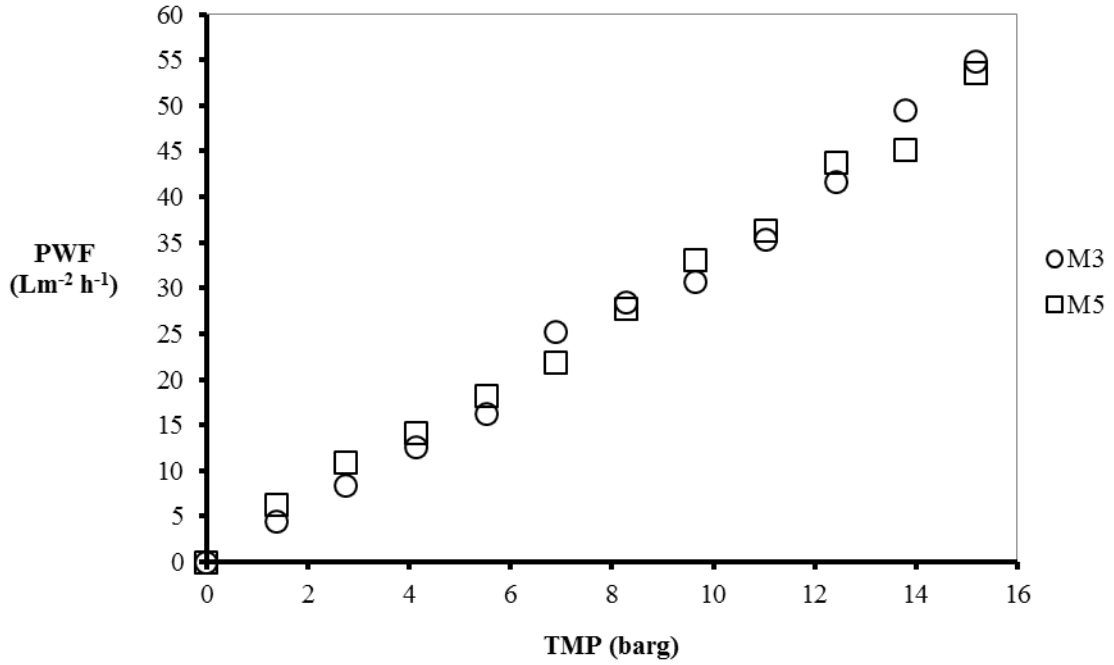

Figure 5. 5 Pure water flux evaluation for M_3 and M_5.

The PWF for M_3 and M_5 at 6.9 bar was measured to be 25.2 L m^{-2} h^{-1} and 21.8 L m^{-2} h^{-1} respectively (see Figure 5.5). The difference between the PWF for M_3 and M_5 is 3.4 L m^{-2} h^{-1}. M_5 has a lower PWF compared to the membranes prepared in Chapter 4, the PWF for M_1 and M_2 at 6.9 bar was measured to be 287.7 L.m^{-2} h^{-1} and 1098.9 L.m^{-2} h^{-1} respectively, indicating that the adoption of CNT dispersion method 3 during MMM preparation resulted in consistent performance for varying CNT particle size. M_5 has a lower PWF compared to the polysulfone membrane, M_4, at 6.9 bar (see Figure 4.13 and Figure 5.5). Increasing the applied pressure enhanced the driving force for permeation, resulting in an increase in the permeation flux (Barona et al., 2013). The FTIR spectra indicated that the functional groups observed for the CNTs included C=O and O−H groups. M_3 and M_5 have a 5% CNT loading, were prepared using

CNT dispersion method 3 and have a similar surface chemistry but the result for the PWF varies. Although the difference in the PWF is not very significant, it can be attributed to the varying particle size. Furthermore, the cross linking density of CNT/polysulfone can be elucidated as very high (Barona et al., 2013), because at the highest TMP, 15.17 bar, the PWF obtained for M_3 and M_5 is still lower when compared to the MMMs prepared in Chapter 4. Further analysis was carried out to evaluate the PWP. The results for M_3 and M_5 are depicted in Table 5.2.

Table 5. 2 The PWP of M_3 and M_5 at varying TMP.

PWP (L m^{-2} $h^{-1}$$bar^{-1}$)		
TMP	M_3	M_5
1.38	3.19	4.49
2.76	3.02	3.96
4.14	3.04	3.40
5.52	2.93	3.29
6.90	3.66	3.16
8.28	3.43	3.34
9.66	3.17	3.42
11.03	3.20	3.29
12.41	3.35	3.52
13.79	3.59	3.27
15.17	3.61	3.53

The PWP for M_3 and M_5 is 3.66 L m^{-2} h^{-1} bar^{-1} and 3.16 L m^{-2} h^{-1} bar^{-1} respectively, at a TMP of 6.9 bar. CNT II particles were used during synthesis of M_5. These CNTs have bigger diameters relative to CNT I samples. Increasing the CNT particle size appears to result in a reduction in the PWF as well as the PWP (see Figure 5.5 and Table 5.2). TEM micrographs of the CNTs confirmed that CNT II particles have shorter lengths than CNT I samples. The cross linking density and interfacial defects have been reported to influence the membrane permeation flux (Barona et al., 2013). This suggests that M_5 has higher cross linking density and lower interfacial defects due to the low CNT surface area present in the polysulfone matrix in the MMM structure.

In the study conducted by Kim et al. (2013), CNT/polysulfone and CNT/polyamide MMMs with MWCNTs were prepared and the PWF evaluated to assess the initial performance. The results obtained in this study have been compared to the findings of Kim et al. (2013) (see Table 5.3). The MWCNT/polysulfone membranes (NLPN) were prepared using the phase inversion method and the MWCNT/polyamide (NHPN) MMMs were prepared by the in-situ interfacial polymerization method according to Kim et al. (2013).

The PWF of NLPN is higher than that of M_3 and M_5 for the given TMP range (2.4 bar to 8.8 bar), the CNT loading for this NLPN was reported to be 10% (which is twice the CNT loading for M_3 and M_5). The pure water permeation flux for polymeric MMMs has been reported to increase with increasing CNT loading (Maphutha et al., 2013). The NHPN MMMs were prepared for high pressure applications and enhanced PWF was obtained for M_3 and M_5 relative to NHPN for TMP greater than 11 bar. This suggests that the polyamide layer formed on the CNT/polysulfone MMM during synthesis affects the performance of the MMMs. Although the

CNT loading for NHPN, M_3 and M_5 is 5%, the effect of the method employed to prepare the MMMs significantly influences the performance of the MMMs (see Table 5.3).

Table 5. 3 PWF study comparison with previous reports for MMMs prepared by Kim et al. (2013).

MMM Materials	**MWCNT/polysulfone**	**MWCNT/polyamide**	**MWCNT/polysulfone**	
CNT Loading (%)	**10**	**5**	**5**	
Refer	**Kim et al. (2013)**	**Kim et al. (2013)**	**This study**	**This study**
TMP (bar)	**NLPN**	**NHPM**	**M_3**	**M_5**
1.38			4.40	6.20
2.40	18.40			
2.76			8.32	10.92
4.00	20.50			
4.14			12.57	14.05
5.12	23.00			
5.52			16.18	18.14
5.76	24.00			
6.90			25.22	21.80
7.20	26.20			
8.28			28.41	27.67
8.80	29.40			
9.66			30.64	33.00

MMM Materials	MWCNT/polysulfone	MWCNT/polyamide	MWCNT/polysulfone	
CNT Loading (%)	10	5	5	
Refer	Kim et al. (2013)	Kim et al. (2013)	This study	This study
TMP (bar)	NLPN	NHPM	M_3	M_5
11.03			35.28	36.32
11.60		18.60		
12.41			41.56	43.68
13.12		19.80		
13.79			49.49	45.11
14.00		23.90		
15.17			54.76	53.57
16.00		25.00		
17.12		28.20		

In order to further evaluate the MMMs, the OWF was measured using the Sterlitech cross flow filtration module at various TMP by Equation (4.1.) The effective membrane area was 42 cm^2. The OWF was measured at room temperature after the membranes were compacted using an oil-water mixture at 8 bar for 4 hours. An emulsified oil and water solution with an oil concentration of 1000 mg/l was prepared by mixing water and diesel using a high speed stirrer for 4 hours. Readings were taken every half an hour with increasing TMP. This initial concentration of 1000 mg/l oil was used in various studies and it is typical of as produced water from oil and gas reservoirs (Chakrabarty et al., 2008). The OWF results are depicted in Figure 5.6.

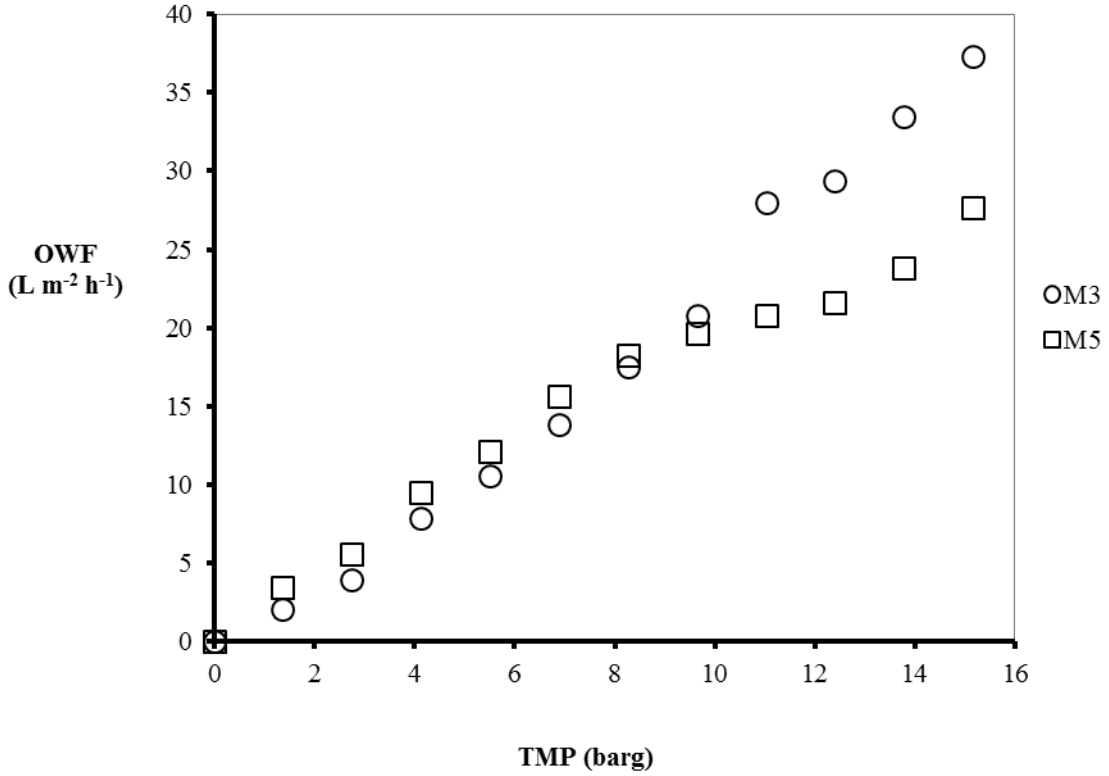

Figure 5. 6 OWF for M_3 and M_5.

The OWF for M_3 and M_5 at 6.9 bar was measured to be 13.8 $L.m^{-2}$ $h^{-1}$and 15.6 $L.m^{-2}$ h^{-1} respectively. The OWF is lower than the PWF for both MMMs for the TMP range in this study. M_3 has a lower OWF below a TMP of 9.66 bar relative to M_5 (see Figure 5.6). Increasing the TMP above 9.66 bar resulted in a decline in the OWF for M_5. This is attributed to initial fouling of the MMM. The measured contact angle for M_3 was 77.3 ± 4.5° and 78.8 ± 5.6° was measured for M_5. Although the difference between the contact angles is 1.5°, the effect on the fouling tendency is significant at high TMP as depicted in Figure 5.6. Further evaluation was carried out to analyse the performance of the MMM and the results of the OWP are depicted in Table 5.4.

Table 5. 4 The PWP for M_3 and M_5 tested at varying TMP.

	OWP (L m^{-2} h^{-1} bar^{-1})	
TMP (bar)	M_3	M_5
1.38	1.46	2.47
2.76	1.41	2.01
4.14	1.88	2.28
5.52	1.91	2.19
6.90	2.00	2.26
8.28	2.11	2.20
9.66	2.15	2.03
11.03	2.53	1.88
12.41	2.36	1.74
13.79	2.42	1.73
15.17	2.46	1.82

The OWP of M_3 is lower to that M_5 below TMP of 9.66 bar but exceeds the OWP for M_5 above this TMP. The observation made is that OWP of M_3 increases with increasing TMP while the OWP for M_5 decreases with increasing TMP above 9.66 bar (see Table 5.4). The PWP and OWF results for the MMMs are depicted in Table 5.5.

Table 5. 5 The PWP and OWP for M_3 and M_5 at varying TMP.

	PWP (L m^{-2} h^{-1} bar^{-1})		**OWP (L m^{-2} h^{-1} bar^{-1})**	
TMP	M_3	M_5	M_3	M_5
1.38	3.19	4.49	1.46	2.47
2.76	3.02	3.96	1.41	2.01
4.14	3.04	3.40	1.88	2.28
5.52	2.93	3.29	1.91	2.19
6.90	3.66	3.16	2.00	2.26
8.28	3.43	3.34	2.11	2.20
9.66	3.17	3.42	2.15	2.03
11.03	3.20	3.29	2.53	1.88
12.41	3.35	3.52	2.36	1.74
13.79	3.59	3.27	2.42	1.73
15.17	15.17	3.61	2.46	1.82

The PWP is higher than the OWP for both membranes as shown in Table 5.5, for TMP from 1.38 bar to 9.66 bar, indicating a decline in the permeability of the MMMs during the separation of oil-water mixture. The decrease in the permeation flux from pure water to oil-water for the MMMs can be attributed to the hydrophilic properties of the MMMs as a result of the presence of oxygen containing functional groups on the CNTs. The decrease in the permeation flux for M_5 for the oil-water solution can be attributed to the higher cross linking of the MMM as well as the

reduced hydrophilic property confirmed by the contact angle. The oil rejection of the MMMs was evaluated using Equation (4.4) (see Figure 5.7).

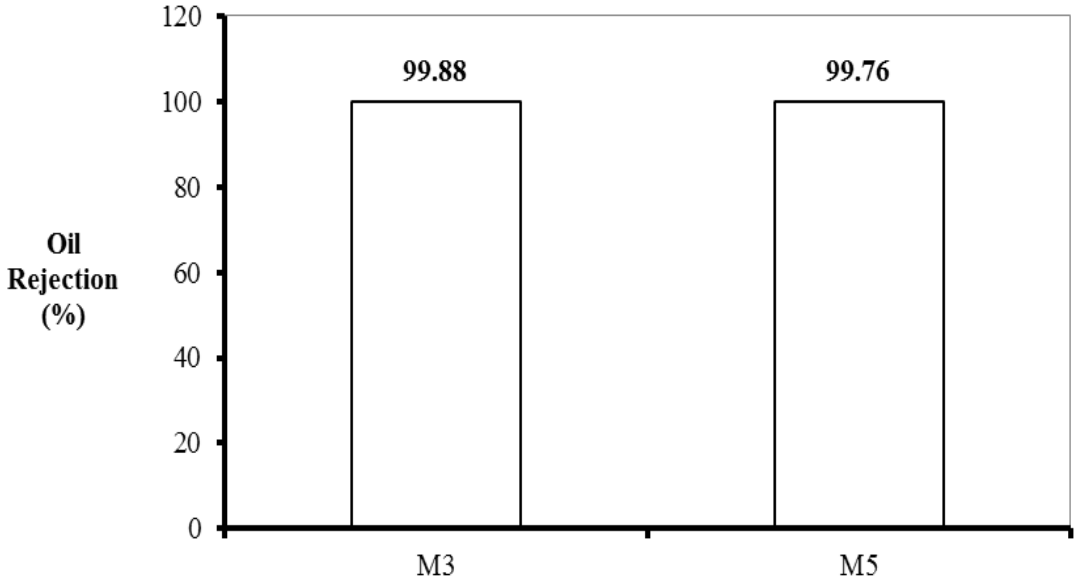

Figure 5.7 The average rejection rate for the membranes for the TMP range.

The highest oil rejection achieved in this study is 99.88% for M_3 as depicted in Figure 5.7. This MMM was observed to have the lowest PWF, PWP, OWF as well as OWP below a TMP of 9.66 bar relative to M_5. The difference in the oil rejection achieved for M_5 and M_3 is 0.12%. The results of the oil rejection for M_3 is higher than the oil rejection calculated for M_1, M_3 and M_4 prepared in Chapter 4 of this study, further proving that CNT dispersion method 3 results in MMM with improved performance in the separation of oil and water. The surface chemistry of the CNT has been shown to be hydrophilic. the FTIR spectra showed the presence of hydroxyl groups, which suggests that MMMs with hydrophilic CNTs in the polymer matrix have a higher

affinity for water as opposed to oil which was demonstrated by the result obtained for M_3 and M_5.

The competition between water and oil to occupy the porous sites on the membranes is one of the factors which can be attributed to oil and water separation, and this appears not to be greatly influenced by the CNT particle size. The CNT diameter difference between CNT I and CNT II samples was 18 times. However this has resulted to an oil rejection difference of 0.12% between M_3 and M_5, which illustrates that CNT particle size does not influence the oil rejection significantly if the CNT diameters are bigger than the molecules targeted for separation. However the effect on the fouling tendencies of the MMMs is higher for bigger CNT particle sizes.

5.4 Summary

MMMs with varying CNT particle size were prepared using CNT dispersion method 3, which was proven to be the best preparation method for synthesizing MMMs in Chapter 4. TEM and FTIR were used to characterize the CNT material and the hydrophilicity of the synthesized MMMs was determined by measuring the contact angle using the sessile drop method. Performance evaluation for the membranes was carried out using a cross flow filtration module to determine the membrane flux and the oil rejection.

CNT dispersion method 3 was adopted during synthesis of MMMs with different CNTs particle sizes, while the CNT loading was kept at 5%. CNT I, OD 6-9 nm **x** L 5 nm, and CNT II, D 110-170 nm **x** L 5-9 μm , was used in this study. The characterisation techniques and performance

evaluation methods used in the Chapter 4 of this work were employed. FTIR spectra confirmed that the functional groups present for both the CNTs are similar and most importantly include carboxylic acid groups (O−H). The contact angles measured for CNT I and II MMMs were 77.3 ± 4.5° and 78.8 ± 5.6° respectively. The oil rejection obtained was 99.88% and 99.76% for CNT I MMMs and CNT II MMMs respectively. The oily water permeability was 2.11 L m^{-2} h^{-1} bar^{-1} and 2.20 L m^{-2} h^{-1} bar^{-1} at 8.28 bar. Fouling of CNT II MMMs commenced at 9.66 bar resulting in a decrease in permeability, while the oil permeation flux for CNT I MMMs increased with increasing TMP above 9.66 bar.

Chapter Six

Conclusions and Recommendations

6 Conclusions and recommendations

6.1 Conclusions

The aim of this study was to determine the best CNT dispersion method out of 3, to be adopted during the synthesis of CNT/polysulfone MMMs and also examine the effect of CNT particle size on the performance of the MMMs in the separation of oil and water mixtures. This was achieved by preparing membranes using the phase inversion method followed by characterising. SEM, TEM were used to characterise the morphology of the CNT samples and membranes while FTIR was the surface chemistry. The hydrophilicity of the synthesized MMMs was determined by measuring the contact angle using the sessile drop method. The performance evaluation for the membranes was carried out using a cross flow filtration module in order to assess the effect the CNT dispersion method adopted during synthesis as well as the CNT particle size on the permeation flux, permeability and the oil rejection during the separation of the oil-water mixtures.

This study demonstrated that the CNT dispersion method employed during membrane synthesis influenced the performance of MMMs in oil and water separation as well as the hydrophilic properties which was evident by the differences in the MMM contact angles obtained. An interesting conclusion is that the incorporation of CNTs in the CNT/polysulfone composites can also be detrimental on the performance of the MMM, which was evident by the poor oil rejection obtained from the MMMs prepared using CNT dispersion method 1 compared to the pure polysulfone results.

Furthermore, the CNT particle size has been shown to influence the performance of CNT/polysulfone MMMs. Increasing the particle size of the CNTs resulted in improved oil permeation flux as well as permeability at low pressure. However, at a TMP above the 8.28 bar, MMMs with bigger CNTs fouled more rapidly. The highest oil rejection obtained in this study is 99.88% for MMMs prepared using CNT I samples. The difference between CNT I and CNT II samples was 18 times, which resulted in an oil rejection difference of 0.12% for the MMMs prepared using these samples, which meant that the CNT particle size did not influence the oil rejection significantly but can mitigate the fouling tendencies of the MMMs in the application of oil-water separation.

6.2 Recommendations for future studies

The recommended activities for future work are the following:

- Previous studies using pristine CNT and a PVA layer on CNT/polysulfone MMM have been reported by Maphutha et al. (2013) to have considerably high rejection in the application of oil and water separation. The recommendation from this work would be to reduce the CNT concentration and add a PVA layer since PVA is relatively affordable when compared to CNT material.
- The employment of the CNT dispersion methods has been shown to affect the performance of the MMM significantly. In future, the effect on the mechanical strength should be investigated.
- A smaller CNT particle size than that which was used in this study can be considered in order to further investigate the effect of CNT particle size on the performance of the MMMs.

- The CNT/polysulfone MMMs must be used with caution for the treatment of formation water samples because the MMMs will dissolve when exposed to solvents/aromatics, which are likely to be present in the formation water.

References

Abadi, S.R.H., Sebzari, M.R., Hemati, M., Rekabdar, F. & Mohammadi, T. (2010).Ceramic performance in microfiltration of oily wastewater. *Desalination, 265,* 222-228.

Abdolmalekia, A, Mallakpoura, S., & Borandeha, S. (2013) Amino acid-functionalized multi-walled carbon nanotubes forimproving compatibility with chiral poly (amide-ester-imide)containing l-phenylalanine and l-tyrosine linkages. *Applied Surface Science, 287,* 117– 123.

Alzahrani, S., Mohammad, A.W., Abdullah, P. & Jaafar, O. (2013) Potential tertiary treatment of produced water using highly hydrophilic nanofiltration and reverse osmosis membranes. *Journal of Environmental Chemical Engineering, 1*, 1341–1349.

Amini, M., Jahanshahi, M. and Rahimpour, A. (2013) Synthesis of novel thin film nanocomposite (TFN) forward osmosis membranes using functionalized multi-walled carbon nanotubes. *Journal of Membrane Science, 435,* 233–241.

Aroon, M.A, Ismaila, A.F, Montazer-Rahmati & M.M., Matsuura, T. (2010). Performance studies of mixed matrix membranes for gas separation: A review. *Separation and Purification technology, 7*5, 229-242.

Barona, G.,N.,B., Lim, J., Choi, M.,& Jong, B. (2013). Interfacial polymerization of polyamide-aluminosilicate SWNT nanocomposite membranes for reverse osmosis. *Desalination, 325, 138–147.*

Chakrabarty, B., Ghoshal, A.K., & Purkait, M.K. (2008).Ultrafiltration of stable oil-in-water emulsion by polysulfone membrane. *J. Membr. Sci., 32*5, 325–427.

Chakrabarty, B., Ghoshal, A., K. & Purkait, M. K. (2010).Cross-flow ultrafiltration of stable oil-in-water emulsion. *Chem. Eng. J., 165*, 447–456.

Cooper, C.A., Ravich, D., Lips, D., Mayer, J. & Wagner, H.D. (2002). Distribution and alignment of carbon nanotubes and nanofibrils in a polymer matrix. Comput.Sci. Technol, 62 1105.

Ebrahimi, M. et al. (2009). Characterization and application of different ceramic membranes for the oil-field produced water separation. *Desalination, 245,* 533–540.

Fu, X., Wang, J., Ding, J., Wu, H., Dong, Y. & Fu, Y. (2013).Quantitative evaluation of carbon nanotube dispersion through scanning electron microscopy micrographs. *Composites Science and Technology, 87,* 170–173.

Han, M.J. & Bhattacharyya, D.(1995). Changes in morphology and transport characteristics of polysulfone membranes prepared by different demixing conditions. *J. Membr. Sci. 98,* 191-200.

Jeong, B.H., Hoek, E.M.V., Yan, Y., Subramani, A., Huang, X., Hurwitz, G… & Jawor, A. (2007). Interfacial polymerization of thin film nanocomposites: A new concept for reverse osmosis membranes. *J.Membr.Sci., 294,* 1–7.

Kim, E, Liu, Y. & El-Din, M.G. (2013). An in-situ integrated system of carbon nanotubes nanocomposite membrane for oils and process-affected water separation. *Journal of Membrane Science, 429,* 418–427.

Kim, E., Hwang, G., El-Din, M.G. & Liu Y. (2012). Development of nanosilver and multi-walled carbon nanotubes thin-film nanocomposite membrane for enhanced water treatment. *Journal of Membrane Science,* 394– 395, 37– 48.

Kołtuniewicz, A.B. (2005). The history and state of art in membrane technologies. Retrieved from: http://www.etseq.urv.es/assignatures/ops/presentacio_membranes.pdf (Accessed 22 August 2014).

Liu, T. X. & Huang, S. (2010). Morphology and thermal behavior of polymer/carbon nanotube composites. *Polymer nanocomposites, 15,* 529-562. Woodhead Publishing Limited

Ma, M., Siddiqui, N.A., Marom, G. & Kim, J.. (2010). Dispersion and functionalization of carbon nanotubes for polymer-based nanocomposites: A review, Part A 41. *Composites,* 1345–1367.

Maphutha, S., Mooth, K., Meyyappan, M. & Iyuke, S.E. (2013).A carbon nanotube-infused polysulfone membrane with polyvinyl alcohol layer for treating oil-containing waste water. *Scientific Reports, 3:1509*. doi:10.1038/srep.

Masuelli, M.A. (2003). Synthesis polysulfone-Acetylethanol Ultrafiltration Membranes. Application to Oily Wastewater Treatment. *Journal of Materials Physics and Chemistry*, 1, 3, 37-44.

McCurry, J. (2008). Organic Chemistry. *Physical Science: David Harris*, 12.7, 425.

Misra, A., Tyagi, P.K., Rai, P. & Misra, D. S. (2007). FTIR Spectroscopy of Multiwalled Carbon Nanotubes: A Simple Approach to Study the Nitrogen Doping. *Journal of Nanoscience and Nanotechnology*, *7*, 1820–1823.

Mondal, S., & Wickramasinghe, S.R. (2008).Produced water separation by nanofiltration and reverse osmosis membranes. J. *Membrane Sci., 322*, 162–170.

Pagidi, A., Saranya, R., Arthanareeswaran, G., Ismail, A.F. & Matsuura, T. (2014) Desalination, 344, 280–288.

Pourfayaz, F., Khodadadi, A.A., Mortazavi, Y. & Jafari S.H. (2010).Plasma functionalization of MWCNTs in He followed by NH_3 treatment and its application in PMMA based nanocomposites, Plasma Process. Polym., 7, 1001–1009.

Petersen, R.J. (1993). Composite reverse osmosis and nanofiltration membranes. *J. Membrane Sci., 83*, 81–150.

Qiu, Y., Zhong, H. & Zhang, Q. (2009). Treatment of stable oil/water emulsion by novel felt-metal supported PVA composite hydrophilic membrane using cross flow ultrafiltration. *Trans. Nonferrous Met. Soc. China*, 19, 773-777

Richards, H.L., Baker, P.G.L. &Iwuoha, E. (2012).Metal Nanoparticle Modified polysulfone Membranes for Use in Wastewater Treatment: A Critical Review. *Journal of Surface Engineered Materials and Advanced Technology, 2*, 183-192.

Sadeghi, I., Aroujalian, A., Raisi, A., Dabir, B., and Fathizadeh, M. (2013) *Journal of Membrane Science, 430*, 24–36.

Shawky, H.A., Chae, S., Lin, S. &Wiesner, M.R. (2011) Synthesis and characterization of a carbon nanotube/polymer nanocomposite membrane for water separation. *Desalination, 272*, 46–50.

Slobodian, P., Svoboda, P., Riha, P., Boruta, R. &Saha, P. (2012).Synthesis of PMMA-co-PMAA copolymer brush on multi-wall carbon nanotubes. *Journal of Surface Engineered Materials and Advanced Technology, 2*, 221-226.

Voicu, S., I, Gales, O., Nechifor, G. &Nechifor, A.C. (2011).Polymer coat improves the detection ability of sensing enzymes. *SPIE newsroom*. Retrieved from: https://www.spie.org/x48500.xml?highlight=x2416&ArticleID=x48500 (Accessed 08 January 2015)

Xie, X., Mai, Y. & Zhou, X. (2005). Dispersion and alignment of carbon nanotubes in polymer matrix: A review. *Materials Science and Engineering, 49*, 89–112.

Yang, Y.K. & Xie, X.L. (2011). Functionalization of carbon nanotubes for polymer nanocomposites. Woodhead Publishing Limited, 55-91.

Yi, X.S., Yu, S.L., Shi, W.X., Sun, N., Jin, L.M., Wang, S... & Sun L.P. (2011) The influence of important factors on ultrafiltration of oil/water emulsion using PVDF membrane modified by nano-sized TiO2/Al2O3.*Desalination, 281,* 179-184.

Yin, J., Zhu, G. & Deng, B. (2013) Multi-walled carbon nanotubes (MWNTs)/polysulfone (PSU) mixed matrix hollow fiber membranes for enhanced water treatment. Journal of Membrane Science, 437, 237–248.

Yudianti, R., Onggo, H., Sudirman, Saito, Y., Iwata, T. & Azuma, J. (2011) Analysis of functional group sited on multi-wall carbon nanotube surface. *The Open Materials Science Journal, 5,* 242-247.

Yu, S., Liu, X., Liu, J., Wu, D., Liu, M. & Gao, C. (2011). Surface modification of thin-film composite Polyamide reverse osmosis membranes with thermo-responsive polymer (TRP) for improved fouling resistance and cleaning efficiency. *Separation and Purification Technology*, *76*, 283–291.

Yu et al. (2013) Improving fouling resistance of thin-film composite polyamide reverses osmosis membrane by coating natural hydrophilic polymer sericin. Separation and Purification Technology, 118, 285–293

Zhao, H., Qiu, S., Wu, L., Zhang, L., Chen, H. & Congjie G. (2014a) Improving the performance of Polyamide reverse osmosis membrane by incorporation of modified multi-walled carbon nanotubes. *Journal of Membrane Science, 450*, 249–256.

Zhao, D., Ren, J., Li, H., Li, X. & Deng, M. (2014b) Gas separation properties of Poly(amide-6-b-ethyleneoxide)/amino modified multi-walled carbon nanotubes mixed matrix membranes. *Journal of Membrane Science, 467*, 41–47.

Appendices

Appendix A Sterlitech membrane test cell system specifications

According to Sterlitech Membrane Test Cell System is designed to evaluate the performance of membranes widely used in Reverse Osmosis, Nanofiltration, and Macrofiltration applications by simulating the flow dynamics of larger, commercially available membrane elements. This tests bench unit offers experimental control by allowing the adjustment of the flow parameters to accommodate a wide range of applications.

Table A. 1 Sterlitech Membrane Test Cell System features and specifications.

Cell type	CF042 (Stainless Steel) 69 barg rated pressure
Number of cells	4
Membrane sample size	5.8 cm ×11.2 cm
Effective membrane area	42 cm^2
Feed flow rate	6 l/m (max)
Feed controls	Bypass valve, Brine/Concentrate Control Valve, Main Power ON/OFF switch
Data display	Digital Display, Max Flow 6.8 l/m, Max Pressure: 69 barg
Operating range	0-69 barg
Electrical supply	208-230 v, 50 Hz , 1- phase
Motor rating	Leeson: 1.5 HP, 8.6 Amps, 1- phase, 1425 RPM
Pump	Hydra-Cell SS diaphragm Type
System dimensions	170 cm ×104 cm × 150 cm
Weight	227 kg
Chiller	PolyScience Digital, 220 V, 50 Hz

Appendix B SEM micrographs of the membranes

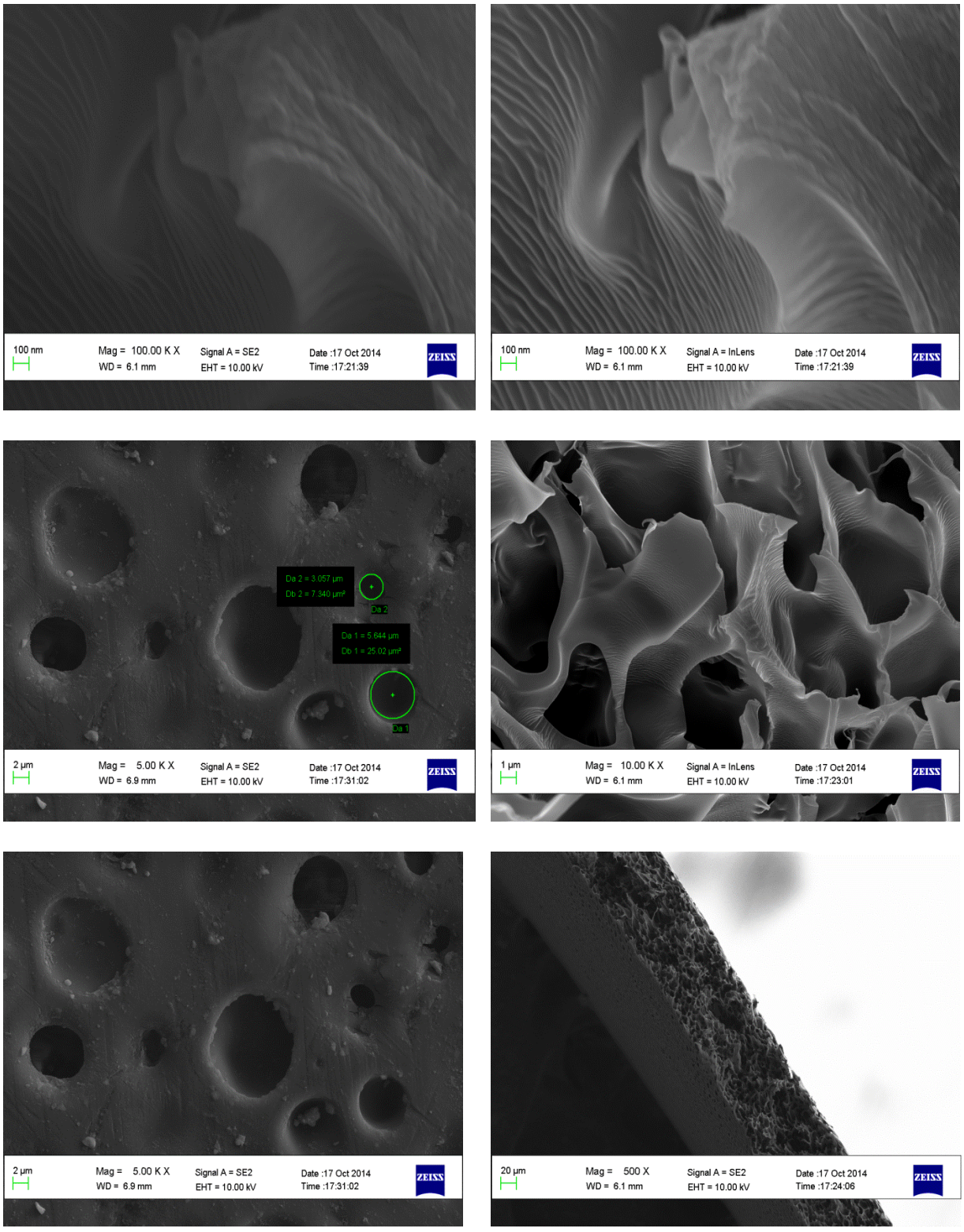

Figure B. 1 SEM images for M_4 MMMs

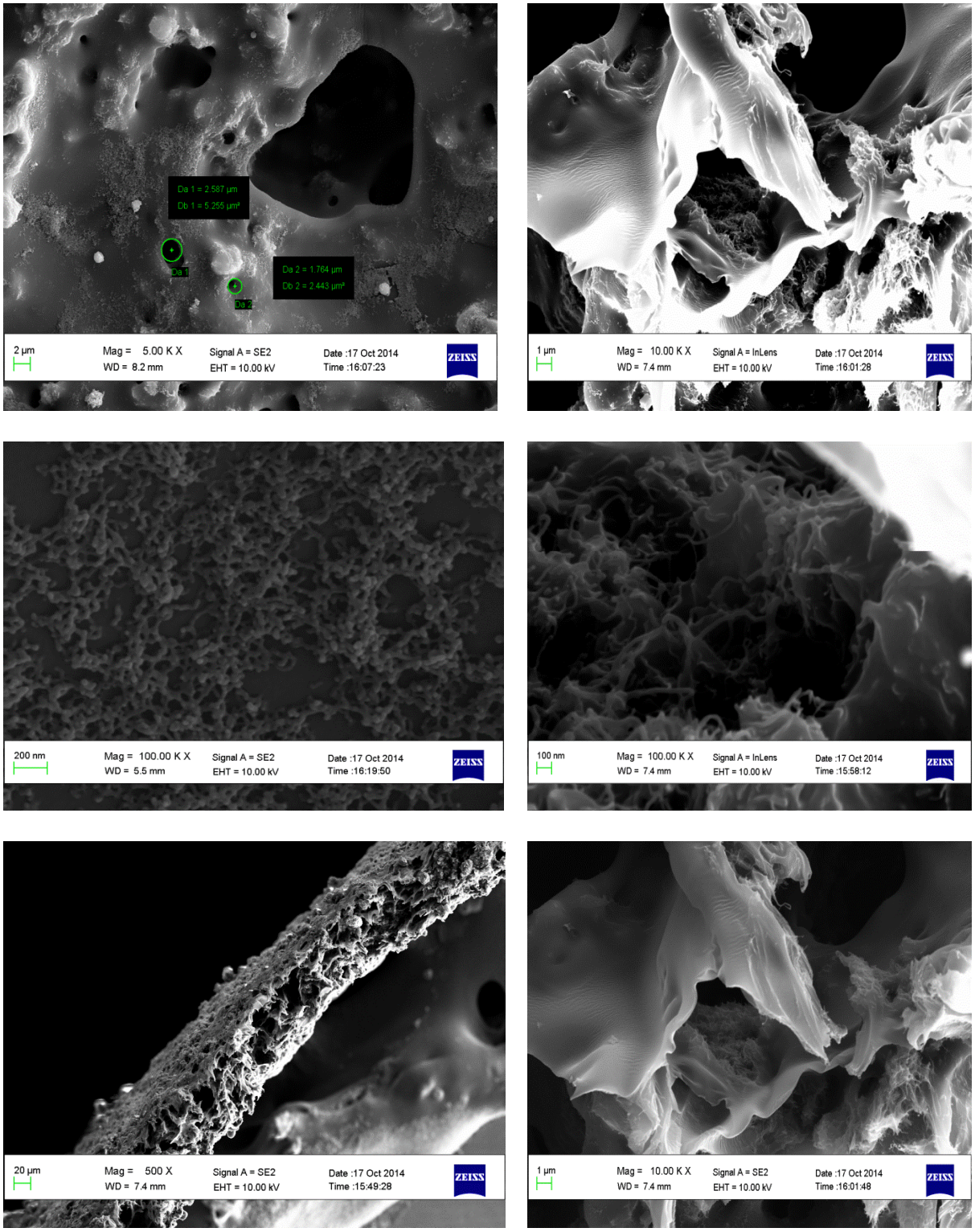

Figure B. 2 SEM images for M_1 MMMs

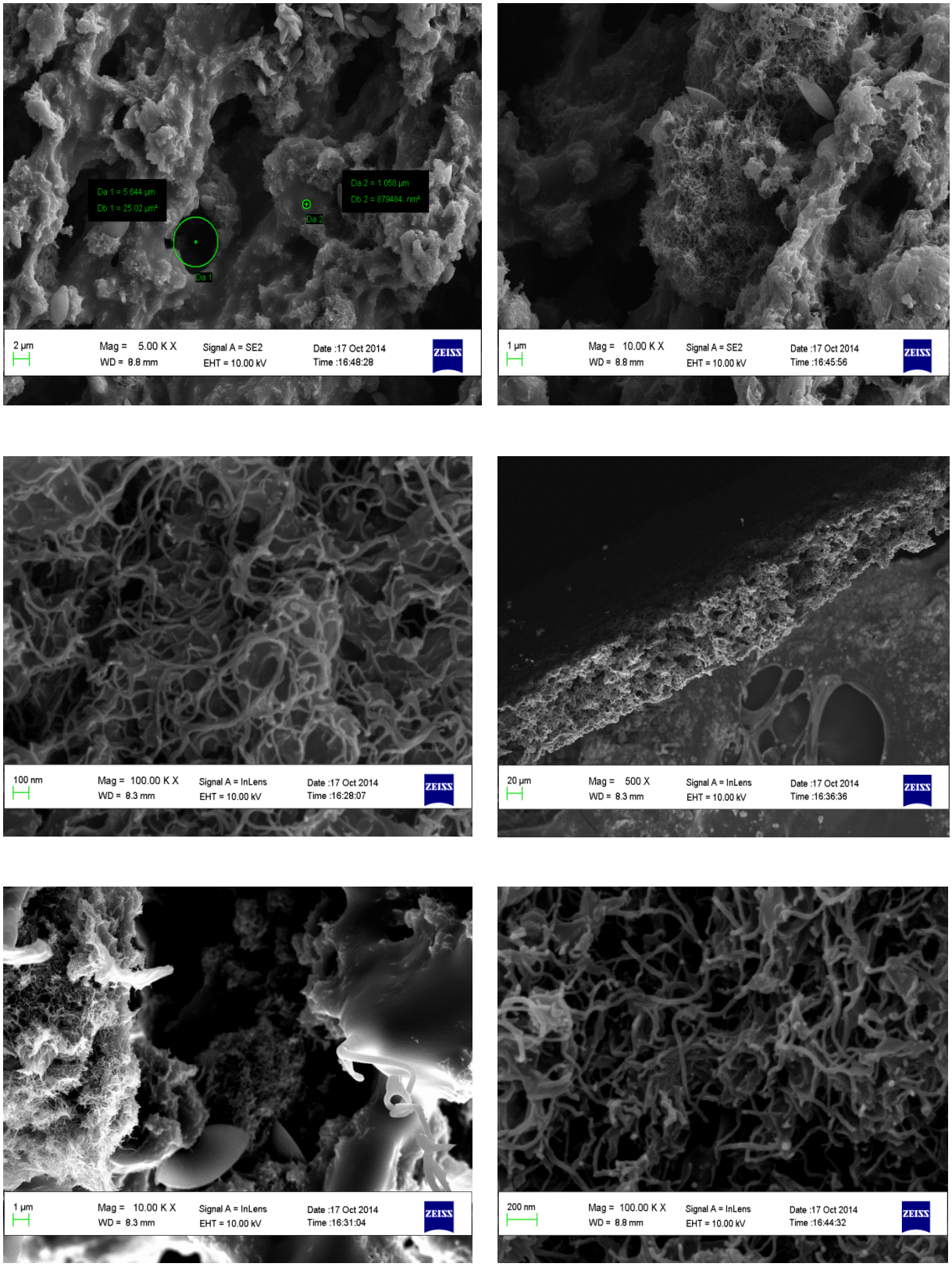

Figure B. 3 SEM images for M_2 MMMs

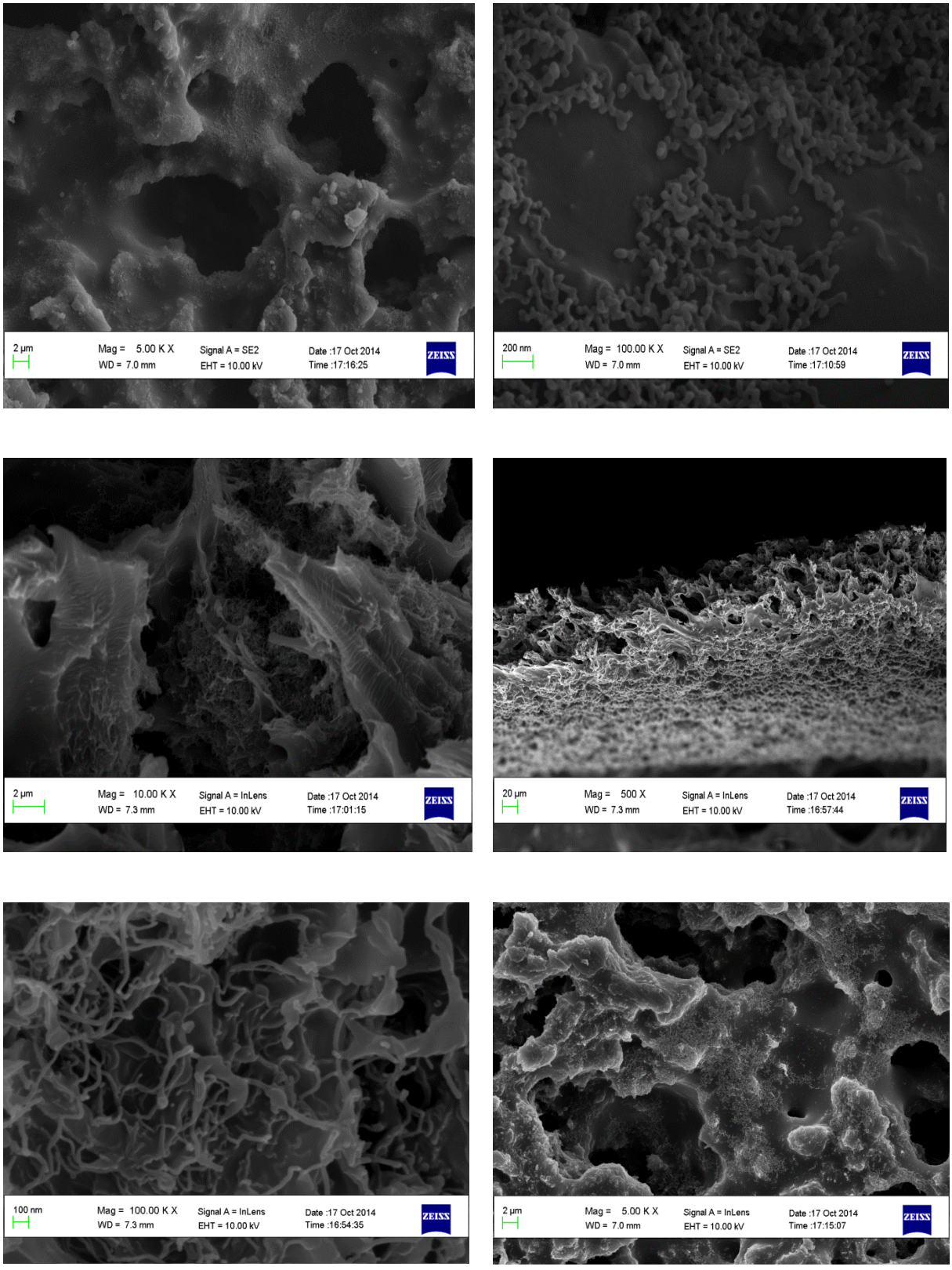

Figure B. 4 SEM images for M_3 MMMs

Appendix C FTIR spectra of the polysulfone polymer (Sigma Aldrich)

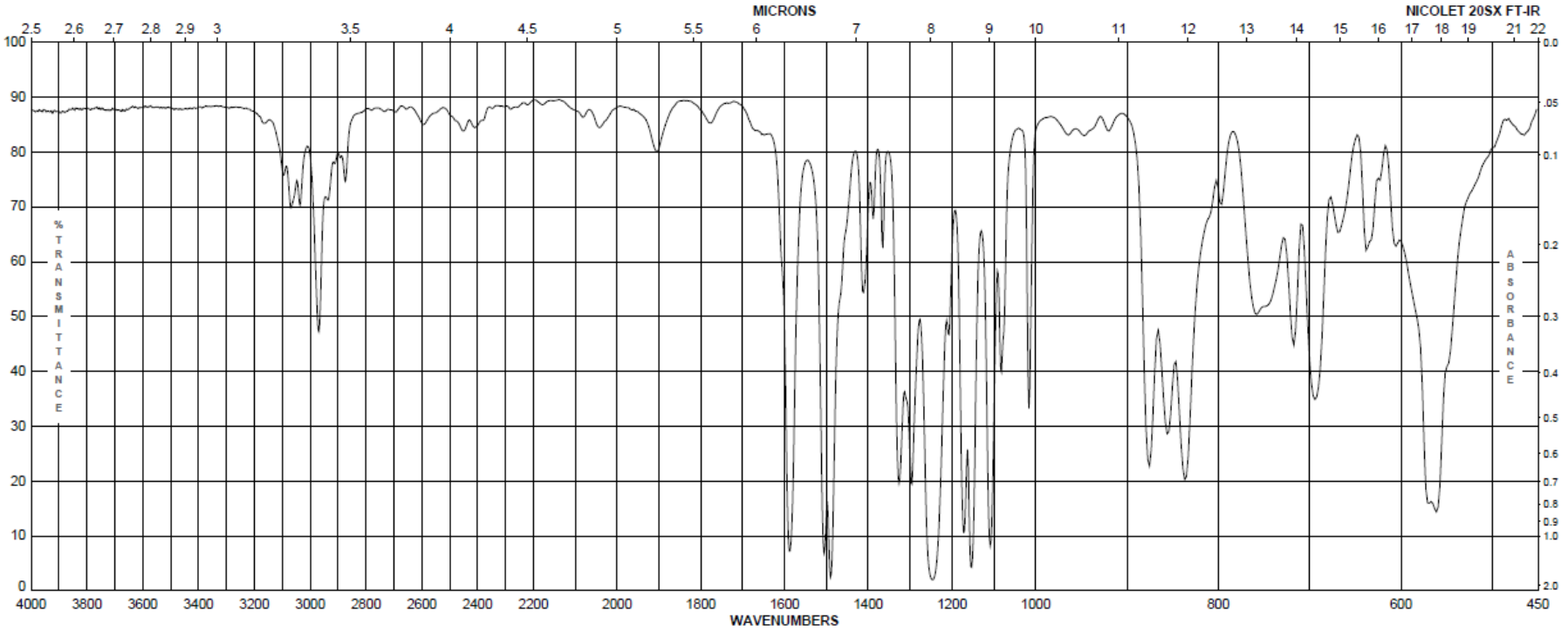

Figure C. 1 FTIR spectra of the polysulfone polymer provided by Sigma Aldrich